UNIVERSIDADE DE BRASÍLIA

PROGRAMA DE PÓS-GRADUAÇÃO EM ZOOLOGIA

Variação morfológica e osteocronologia do clado de *Trachycephalus nigromaculatus* (sensu Blotto et al., 2021) (Anura: Hylidae: Lophyohylini)

Isabella Parreira dos Santos

Brasília
Maio/2024

UNIVERSIDADE DE BRASÍLIA

PROGRAMA DE PÓS-GRADUAÇÃO EM ZOOLOGIA

Variação morfológica e osteocronologia do clado de *Trachycephalus nigromaculatus* (*sensu* Blotto et al., 2021) (Anura: Hylidae: Lophyohylini)

Isabella Parreira dos Santos

Dissertação de Mestrado apresentada ao Programa de Pós-graduação em Zoologia, Instituto de Ciências Biológicas, da Universidade de Brasília, como parte dos requisitos necessários à obtenção do título de Mestre em Zoologia.

Orientador(a): Prof. Dr. Reuber Albuquerque Brandão.

Brasília

Maio/2024

Trachycephalus mambaiensis. Arinos, Minas Gerais.

Variação morfológica e osteocronologia do clado de *Trachycephalus nigromaculatus* (*sensu* Blotto et al., 2021) (Anura: Hylidae: Lophyohylini)

Isabella Parreira dos Santos

Orientador: Prof. Dr. Reuber Albuquerque Brandão

Dissertação de Mestrado apresentada ao Programa de Pós-graduação em Zoologia, Instituto de Ciências Biológicas, da Universidade de Brasília, como parte dos requisitos necessários à obtenção do título de Mestre em Zoologia.

Aprovada por
(Reuber Albuquerque Brandão) Presidente – UnB
(Manoela Woitovicz Cardoso) – MNRJ
(Boris Leonardo Blotto) – MACN

Brasília
Maio/ 2024

Ficha catalográfica elaborada automaticamente, com os dados fornecidos pelo(a) autor(a)

```
        Parreira dos Santos, Isabella
PP259v     Variação morfológica e osteocronologia do
        clado de Trachycephalus nigromaculatus (sensu
        Blotto et al., 2021) (Anura: Hylidae:
        Lophyohylini) / Isabella  Parreira dos Santos;
        orientador Reuber Albuquerque Brandão. --
        Brasília, 2024.
           75 p.


           Dissertação(Mestrado em Zoologia) -- Universidade de
        Brasília, 2024.


           1. anatomia do crânio. 2. anéis de crescimento anual. 3.
        morfometria geométrica. 4. sazonalidade. 5. tamanho do
        corpo. I. Albuquerque Brandão, Reuber, orient. II. Título.
```

Agradecimentos

Aos amigos e amigas, que também são minha equipe de campo e laboratório:

Afonso Meneses
Anderson Kennedy de Lima
Emayre Rebecca Campos
Fernanda Barros Passaglia
Luis Felipe de Lima
Murielly Coimbra
Pedro Paulo de Queiroz

Aos pesquisadores e pesquisadora que me acolheram como aluna nas coleções onde tive o privilégio de visitar:

Guarino Colli – Coleção Herpetológica da Universidade de Brasília (CHUNB/UnB)
Renato Feio – Museu de Zoologia João Moojen
José P. Pombal Jr. – Museu Nacional do Rio de Janeiro (MNRJ)
Ulisses Caramaschi – Museu Nacional do Rio de Janeiro (MNRJ)
Manoela Woitovicz Cardoso – Museu Nacional do Rio de Janeiro (MNRJ)
Thiago Ribeiro Carvalho – Coleção Herpetológica da Universidade Federal de Minas Gerais (UFMG)

Aos demais pesquisadores e pesquisadoras que apoiaram este projeto de alguma forma:

Renato Gomes Faria – Universidade Federal de Sergipe (UFS)
Flora Juncá – Museu de Zoologia de Feira de Santana (UEFS)
Célio F. B. Haddad – Universidade Estadual Paulista (UNESP)
Nadya Carolina Pupin – Universidade Estadual Paulista (UNESP)
Victor Dill Orrico – Universidade Estadual de Santa Cruz (UESC)
Tadeu Medeiros – Universidade Estadual de Santa Cruz (UESC)
Elisa Freire – Universidade Federal do Rio Grande do Norte (UFRN)

Ao meu laboratório favorito neste mundo e seu coordenador, e meu orientador:

Laboratório de Fauna e Unidades de Conservação (LAFUC)
Reuber Albuquerque Brandão

Equipes de fomento

CAPES – Coordenação de Aperfeiçoamento de Pessoal de Nível Superior – Bolsa de Mestrado

FAPDF – Financiamento à Pesquisa do Distrito Federal

PROAP (PPGZOO) – Edital 04/2022

DPG – Edital 0005/2022 – Bolsa de Mestrado

UNB – Gasolina para a kombi

PPGZOO – Programa de Pós-Graduação em Zoologia

SISBIO – Licença Científica nº 867664-1

Sumário

RESUMO

Variação morfológica e osteocronologia do clado de *Trachycephalus nigromaculatus* (*sensu* Blotto et al., 2021) (Anura: Hylidae: Lophyohylini)

Isabella Parreira dos Santos
Orientador: Prof. Dr. Reuber Albuquerque Brandão

Resumo da Dissertação de Mestrado apresentada ao Programa de Pós-graduação em Zoologia, Instituto de Ciências Biológicas, da Universidade de Brasília, como parte dos requisitos necessários à obtenção do título de Mestre em Zoologia.

Com o objetivo de investigar a variação morfológica e o atual status taxonômico do clado composto por *Trachycephalus nigromaculatus*, *T. atlas* e *T. mambaiensis*, analisamos as medidas morfométricas do corpo, e a forma e anatomia do crânio por meio da morfometria geométrica. Encontramos diferenças morfológicas significativas entre as espécies, evidenciadas por análises discriminantes lineares (LDA) e análises de variância (Anova). Também identificamos dimorfismo sexual no tamanho do corpo e nas medidas da cabeça nas três espécies estudadas. As análises de componentes principais (PCA) da morfometria geométrica revelaram variações significativas na forma craniana entre as espécies, destacando diferenças na largura do crânio, comprimento e posição da premaxila, comprimento e posição do esquamosal, comprimento e posição do prootico, largura do frontoparietal, e comprimento e largura do paraesfenoide. Observamos diferenças nos níveis de hiperossificação em indivíduos da mesma espécie e diferenças anatômicas distintas entre as espécies, incluindo variações na forma e articulação de elementos cranianos, tais como o frontoparietal e esquamosal. Também investigamos a relação entre o tamanho do corpo e a idade dos espécimes através de osteocronologia, bem como o padrão de atividade anual das três espécies. A estimativa de idade através da contagem de anéis de crescimento (LAGs) revelou disparidades na idade estimada, maturidade sexual e curvas de crescimento entre as espécies. Machos de *T. nigromaculatus* e *T. atlas* atingiram maturidade sexual com duas LAGs, enquanto machos de *T. mambaiensis* com uma LAG. Observamos correlações significativas entre o comprimento rostro-cloacal (SVL) e a idade para *T. nigromaculatus* e *T. atlas*, mas não para *T. mambaiensis*. *Trachycephalus atlas* exibiu crescimento mais lento em comparação com *T. nigromaculatus.* Espécimes de *T. nigromaculatus* foram encontrados durante quase todo o ano, enquanto *T. atlas* e *T. mambaiensis* foram encontrados principalmente durante a estação chuvosa. Esses achados sugerem divergência nos padrões de crescimento, mas tendência ao comportamento sazonal entre as espécies. Nossos resultados aprofundam nossa compreensão sobre a diversidade morfológica e taxonomia do gênero *Trachycephalus*, especialmente sobre processos evolutivo-ecológicos e história natural de *Trachycephalus* a partir de espécimes preservados em museus.

Palavras-chave: anatomia do crânio, anéis de crescimento anual, morfometria geométrica, sazonalidade, tamanho do corpo.

Brasília
Maio/2024

ABSTRACT

Variação morfológica e osteocronologia do clado de *Trachycephalus nigromaculatus* (*sensu* Blotto et al., 2021) (Anura: Hylidae: Lophyohylini)

Isabella Parreira dos Santos
Orientador: Prof. Dr. Reuber Brandão

Abstract da Dissertação de Mestrado apresentada ao Programa de Pós-graduação em Zoologia, Instituto de Ciências Biológicas, da Universidade de Brasília, como parte dos requisitos necessários à obtenção do título de Mestre em Zoologia.

Title: Morphological Variation and Skeletochronology of the clade of *Trachycephalus nigromaculatus* (sensu Blotto et al., 2021) (Anura: Hylidae: Lophyohylini).

We investigated the variation and taxonomic status of *Trachycephalus nigromaculatus, T. atlas,* and *T. mambaiensis*. We employed geometric morphometrics to analyze skull and we analyzed the variation of morphometric measurements between species. Significant morphological differences among the species were identified through linear discriminant analyses and analyses of variance (ANOVA). We observed female-biased sexual dimorphism in body size and head measurements in the three species. Principal component analyses (PCA) of geometric morphometrics highlighted significant variations in cranial shape, particularly in skull width, premaxilla length and position, squamosal length and position, prootic length and position, frontoparietal width and, parasphenoid length and width. We observed different degrees of ossification within species and distinct anatomical characteristics, including variations in cranial elements such as the frontoparietal and squamosal. The relationship between body size and age was assessed using osteochronology, and we observed differences in estimated age, sexual maturity, and growth curves among the species. Males of *T. nigromaculatus* and *T. atlas* reached sexual maturity with two growth rings, while *T. mambaiensis* males reached maturity with one. We found correlations between snout-vent length (SVL) and age for *T. nigromaculatus* and *T. atlas*, but not for *T. mambaiensis*. *Trachycephalus atlas* exhibited slower growth compared to *T. nigromaculatus*. Specimens of *T. nigromaculatus* were present throughout most of the year, whereas

T. atlas and *T. mambaiensis* were primarily found during the rainy season. These findings suggest divergent growth patterns but a tendency towards seasonal behavior among the species. This study contributes to our understanding of the morphological diversity and taxonomy of the genus *Trachycephalus*, particularly regarding evolutionary-ecological processes and natural history based on museum specimens.

Key Words: age, annual record, body size, cranial osteology, geometric morphometrics, skeletochronology.

Brasília
Maio/2024

Introdução Geral

A complexa relação entre tamanho corporal, padrões de crescimento e idade em anuros reflete suas estratégias de história de vida e adaptações ecológicas (Morrison & Hero 2003, Liao et al. 2016), as quais, por sua vez, são influenciadas por fatores evolutivos, genéticos e ambientais (Castanet 1993, Feilich 2016). Essas características desempenham papéis cruciais na biologia dos anuros, afetando aspectos como distribuição, preferências de habitat, maturidade sexual e dinâmica de taxa de crescimento (Arantes et al. 2015; Rebouças et al. 2019; Baraquet et al. 2021). O crescimento em anuros geralmente é contínuo e reflete correlações entre o tamanho corporal e a idade (Halliday & Verrell 1988; Li et al. 2010; Arantes et al. 2015, Otero et al. 2017a, 2017b), parâmetros essenciais para compreender diversos processos evolutivos e ecológicos (Halliday & Verrell 1988, Li et al., 2010, Arantes et al., 2015, Otero et al., 2017a; 2017b).

Nesse contexto, a presença das Linhas de Crescimento Interrompido (LAG) nos tecidos ósseos desempenha um papel fundamental na análise das dinâmicas de crescimento e idade em espécies de anuros (Sinsch 2015). A formação das LAGs decorre de um ritmo circanual geneticamente determinado, o qual é reforçado e sincronizado por variações sazonais (Castanet et al., 1993). Essas linhas funcionam como marcadores temporais, evidenciando a dinâmica do crescimento individual (Castanet et al., 1993).

Além do tamanho do corpo, demais variáveis morfológicas externas são essenciais para a compreensão do papel da ecologia e evolução das características físicas de um organismo (Wiens 2001). O comprimento e a largura da cabeça refletem sua morfologia, e sofre pressões seletivas por abrigar os órgãos sensoriais, capturar presas, fornecer proteção e participar da locomoção e reprodução dos indivíduos (Parmelee 1999, Barros et al., 2011, Paluh et al. 2020).

O sexo também é um fator biológico de interesse intrínseco para explicar a variação morfológica da cabeça (Sanches et al. 2022), uma vez que as medidas cranianas muitas vezes são sexualmente dimórficas em tamanho e forma nos anuros (Arantes et al., 2015, Melo-Moreira et al., 2021). Esses traços dimórficos podem ser resultado de processos microevolutivos tanto reprodutivos quanto não reprodutivos (Katsikaros & Shine, 1997) e comumente variam através de padrões de desenvolvimento alométrico (Fairbairn 1997, Birch 1999).

A alometria é um importante vetor de diversificação morfológica na natureza (Klingenberg 2016), revelando a correlação entre discrepâncias na taxa de crescimento entre diferentes partes do corpo (Huxley 1932, 1924). Diferentes níveis de variação de tamanho podem ser explorados por meio de abordagens integradas, incluindo investigações sobre variações de tamanho interespecíficas em um único estágio ontogenético (alometria estática), com base em indivíduos adultos de uma mesma população (Drake & Klingenberg 2008, Spradley & Jantz 2011) ou entre espécies intimamente relacionadas (Ivanović et al., 2007). Mesmo em um único estágio ontogenético, o tamanho do corpo varia consideravelmente entre os organismos, influenciando a evolução da forma do crânio (Callery & Elinson 2000).

Em contraste, a osteologia do crânio é geralmente considerada conservadora evolutivamente, desempenhando importante papel na taxonomia dos anuros (Trueb 1973). A forma do crânio está geralmente correlacionada com o tamanho do corpo (Trueb & Alberch, 1985), a biologia alimentar (Emerson 1985) e o uso de micro-habitat (Trueb 1973; 1993, Bardua et al. 2021). Algumas espécies de anuros apresentam hiperossificação do crânio, que pode ser expressa pelo surgimento de padrões ornamentações nos ossos dermais (exostose, Pombal et al. 2003, Buffrenil et al. 2016), pela expansão de ossos dermais formando crânios como capacetes (casquing, Trueb 1970a), e pela co-ossificação entre o osso e a derme (Trueb 1970a, 1973, Jared et al., 2005). A co-ossificação no crânio está possivelmente relacionada à fragmose (Trueb 1970; 1973; 1993) e ao equilíbrio hídrico em micro-habitat áridos (Andrade & Abe 1997, Navas et al., 2002).

A tribo Lophyohylini é um clado monofilético de Hylidae, reconhecida por diversas sinapomorfias moleculares (Blotto et al., 2021) e que agrupa espécies com mecanismos antipredatórios, larvas com modificações relacionadas à oofagia e diferentes graus de hiperossificação do crânio (Faivovich et al. 2005, Blotto et al. 2021). Uma putativa sinapomorfia morfológica da tribo é a presença de pelo menos quatro fileiras de dentes labiais posteriores no disco oral do girino (Faivovich et al., 2005). A tribo compreende 89 espécies descritas em oito gêneros sendo *Corythomantis* (2 spp.), *Dryaderces* (2 spp.), *Itapotihyla* (monotípico), *Nyctimantis* (7 spp.), *Osteocephalus* (27 spp.), *Osteopilus* (8 spp.), *Phyllodytes* (15 spp.), *Phytotriades* (monotípico), *Tepuihyla* (9 spp.) e *Trachycephalus* (18 spp.) (Blotto et al. 2021, Frost 2024), presentes na América do Sul e Índias Ocidentais (Faivovich et al., 2005).

O clado formado por *Trachycephalus nigromaculatus* Tshudi, 1838, *T. atlas* Bokermann, 1966, e *T. mambaiensis* Cintra, Silva, Silva, Garcia, & Zaher, 2009, compreende pererecas-de-capacete pouco estudadas do ponto de vista ecológico e taxonômico. *Trachycephalus nigromaculatus* possui ampla distribuição, incluindo restinga na Mata Atlântica no estado do Espírito Santo e no Rio de Janeiro, transição Mata Atlântica-Cerrado no estado da Bahia, e fragmentos florestais de Cerrado no estado de Minas Gerais, Goiás e Piauí (Almeida et al., 2011; Lutz, 1954; Freitas & Lima, 2009; Dias et al., 2010; Martins & Assalim, 2019). Todos os registros conhecidos de *Trachycephalus atlas* são do nordeste do Brasil, incluindo floresta tropical úmida no estado de Pernambuco, matas secas dos estados do Ceará, Sergipe, Alagoas e Paraíba, e na restinga do estado da Bahia (Borges-Nojosa & Arzabe, 2005; Roberto et al., 2011; Neta et al., 2018; Magalhães et al., 2011; Gondim-Silva et al., 2016). Até agora, poucos registros são conhecidos para *Trachycephalus mambaiensis,* todos exclusivamente no Cerrado, incluindo os estados de Minas Gerais, Goiás, Tocantins e Bahia (Silveira & Pacheco 2001, Freitas et al. 2011 Dayrell et al. 2012, Vaz-Silva et al. 2020, Silva et al. 2020).

O clado de *Trachycephalus nigromaculatus* apresenta morfologia externa conservada e as espécies diferem por elementos anatômicos e graus de hiperossificação do crânio (Bokermann, 1966; Trueb, 1970a; Cintra et al., 2009). *Trachycephalus mambaiensis* possui frontoparietais que não cobrem os proóticos posteriormente e ausência de um entalhe pré-maxilar medial no crânio (Cintra et al., 2009). *Trachycephalus atlas* difere de *T. nigromaculatus* pela cabeça mais longa que larga, cristas frontoparietais mais longas e maior distância interorbital (Trueb, 1970; Bokermann, 1966). *Trachycephalus nigromaculatus* e *T. mambaiensis* diferem de *T. atlas* pela presença, durante a vida, de manchas avermelhadas pequenas ou médias dispersas no dorso (Bokermann, 1966; Cintra et al., 2009). Além disso, as divergências genéticas entre as espécies são baixas e há uma linhagem parafilética dentro do clado (Blotto et al. 2021), indicando a necessidade de uma revisão morfológica a fim de compreender o atual status taxonômico das diferentes linhagens que compõem o grupo.

Objetivo Geral

Considerando a baixa divergência genética e a morfologia externa conservada entre suas linhagens, é possível que ocorram identificações equivocadas das espécies que compõem o clado formado por *Trachycephalus nigromaculatus, T. atlas* e *T. mambaiensis.* Desta forma, através de abordagens morfológicas e anatômicas, visamos avaliar o status taxonômico e comparar a história de vida dessas espécies.

Objetivos Específicos

- Explorar a diversidade intraespecífica da forma do crânio por meio da morfometria geométrica.
- Descrever o crânio de *Trachycephalus atlas.*
- Comparar a morfologia do crânio entre as espécies.
- Explorar a história de vida das espécies utilizando a osteocronologia e o tamanho do corpo.

Referências bibliográficas

Almeida A de P, Gasparini JL, Peloso PLV. 2011. Frogs of the state of Espírito Santo, southeastern Brazil - The need for looking at the 'coldspots'. Check List, 7(4): 542- 560.

Arantes IC, Vasconcellos MM, Boas TCV, Veludo LBA, Colli GR. 2015. Sexual Dimorphism, Growth, and Longevity of Two Toad Species (Anura, Bufonidae) in a Neotropical Savanna. Copeia103, No. 2, 2015, 329–342.

Baraquet M, Pollo FE, Otero MA, Grenat PR, Salas NE, Martino AL. 2021. Body size, age and growth in males' populations of *Boana pulchella* (Anura, Hylidae). Anais da Academia Brasileira de Ciências, 93 (4).

Barros FC, Herrel A., Kohlsdorf T. 2011. Head shape evolution in Gymnophthalmidae: Does habitat use constrain the evolution of cranial design in fossorial lizards?J. Evol.Biol.24, 2423–2433.

Birch JM. 1999. Skull allometry in the marine toad, *Bufo marinus*. Journal of Morphology 241: 115-126

Blotto BL, Lyra ML, Cardoso MC, Trefaut Rodrigues M, Dias RI, Marciano-Jr E, Dal Vechio F, Orrico VG, Brandão RA, Lopes de Assis C, Lantyer-Silva AS, Rutherford MG, Gagliardi-Urrutia G, Solé M, Baldo D, Nunes I, Cajade R., Torres A, Grant T, Jungfer K.-H, da Silva HR, Haddad CF, Faivovich J. 2021. The phylogeny of the Casque-headed Treefrogs (Hylidae: Hylinae: Lophyohylini). Cladistics, 37: 36-72.

Bokermann WCA. 1966. Una nueva especie de *Trachycephalus* de Bahia, Brasil (Amphibia, Hylidae). Neotropica. La Plata 12: 120–124.

Borges-Nojosa DM, Arzabe C. 2005. Diversidade de anfíbios e répteis em áreas prioritárias para a conservação da caatinga. In Análise das variações da biodiversidade do bioma caatinga: suporte a estratégias regionais de conservação (F. S. Araújo, M. J. N. Rodal & M. R. V. Barbosa, eds.). Ministério do Meio Ambiente, Secretaria de Biodiversidade e Florestas, Brasília, p.227-241.

Caramaschi, U. & Silvano, D. 2004. *Trachycephalus atlas*. The IUCN Red List of Threatened Species 2004. Electronic Database accessible at. Downloaded on 08 june 2023.

Castanet JH, Francillon-Vieillot, F. J. Meunier, Ricqlès A. de. 1993. Bone and individual aging 7: 245–283 in B. K. Hall (ed.), Bone: Bone Growth. Boca Raton. CRC Press.

Cintra CED, Silva HLR, Silva NJ, Garcia Jr. PC de A, Zaher H. 2009. A new species of *Trachycephalus* (Amphibia, Anura, Hylidae) from the state of Goiás, Brazil. Zootaxa 1975: 58– 68.

Dayrell JS, Fernandes VD, Moura MR, Feio RN. 2012. New records of *Trachycephalus mambaiensis* (Amphibia: Hylidae) from a cerrado region in Minas Gerais state, Brazil. Check List 8(2): 269-271.

Dias IR, Vilaça TRA, Silva JRS, Barbosa RS, Solé M. 2010. Amphibia, Anura, Hylidae, *Trachycephalus nigromaculatus* Tschudi, 1838: Distribution extension. Check List, 6(3): 212-213.

Drake A, Klingenberg C. 2007. The pace of morphological change: historical transformation of skull shape in St Bernard dogs. Proceedings of the Royal Society BBiological Sciences. Proceedings. Biological sciences / The Royal Society. 275. 71-6. 10.1098/rspb.2007.1169.

Faivovich J, Haddad CFB, Garcia ACP, Frost RD, Campbell AJ, Wheeler CW. 2005. Systematic review of the frog family Hylidae, with special reference to Hylinae: a phylogenetic analysis and taxonomic revision. Bulletin of the American Museum of Natural History, 294: 1– 240.

Fairbairn DJ. 1997. Allometry for sexual size dimorphism: pattern and process in the coevolution of body size in males and females. Annual Review of Ecology and Systematics 28(1): 659-687.

Feilich KL. 2016. Correlated evolution of body and fin morphology in the cichlid fishes. Evolution, 70: 2247–2267. https://doi.org/10.1111/evo.13021.

Freitas MA, Lima TO. 2009. *Trachycephalus nigromaculatus* (Blackspotted Casque-headed Tree Frog). Herpetological Review 40(3): 363.

Frost DR. Amphibian Species of the World: An Online Reference. Version 5.5 (abril, 2024). Electronic Database on https://amphibiansoftheworld.amnh.org/.

Gondim-Silva F, Andrade A, Abreu R, Nascimento J, Corrêa G, Menezes L, Trevisan C, Camargo S, Napoli M. 2016. Composition and diversity of anurans in the Restinga of the Conde municipality, Northern coast of the state of Bahia, Northeastern Brazil. Biota Neotropica. 16. 1-16. 10.1590/1676-0611-BN-2016-0157.

Halliday TR, Verrell PA. 1988. Body Size and Age in Amphibians and Reptiles. Journal of Herpetology, 22 (3), 253–265.
Huxley J. 1924. Applied biology. Rice Institute Pamphlet-Rice University Studies, 11(4).

Huxley JS. 1932. Problems of Relative Growth. The Johns Hopkins University Press, Baltimore.

Ivanović A, Vukov TD, Džukić G, Tomaševič N, Kalezić ML. 2007. Ontogeny of skull size and shape changes within a framework of biphasic lifestyle: a case study in six *Triturus* species (Amphibia, Salamandridae). – Zoomorphology 126: 173–183.

Katsikaros K, Shine R. 1997. Sexual dimorphism in the tusked frog, *Adelotus brevis* (Anura: Myobatrachidae): the roles of natural and sexual selection. Biol. J. Linn. Soc. 60, 39e51. https://doi.org/10.1006/bijl.1996.0087.

Klingenberg CP, Duttke S, Whelan S, Kim M. 2016. Developmental plasticity, morphological variation and evolvability: a multilevel analysis of morphometric integration in the shape of compound leaves. J Evol Biol 25:115–129

Liao WB, Luo Y, Lou SL, Jehle R. 2016. Geographic variation in life-history traits: growth season affects age structure, egg size and clutch size in Andrew's toad (*Bufo andrewsi*). Front Zool 13, 6. https://doi.org/10.1186/s12983-016-0138-0

Li C., Liao WB, Yang ZS, Zhou CQ. 2010. A skeletochronological estimation of age structure in a population of the Guenther's frog, Hylarana guentheri, from western China. Acta Herpetologica, 5, 1–11.

Lutz B. 1954. Anfíbios anuros do Distrito Federal. Memórias do Instituto Oswaldo Cruz, 52(1): 155-216.

Magalhães AJC Jr, Barbosa AR, Azevedo SM Jr, Pinho MS, Beltrão MG, Freire BC. 2011. Amphibia, Anura, Hylidae, *Trachycephalus atlas* Bokermann, 1966: Novo registro e comentários sobre a distribuição geográfica. Revista Nordestina de Zoologia Recife, 5(2): 53-57.

Martins RA, Assalim AM. 2019. First record of *Trachycephalus nigromaculatus* (Amphibia, Anura, Hylidae) in the state of Piauí, Brazil. Check List 15(3): 411-414.

Melo-Moreira DA, Murta-Fonseca RA, Galdino CAB, Nascimento LB. 2021. Does a male nest builder have the same head shape as his mate? Sexual dimorphism in Leptodactylus fuscus (Anura: Leptodactylidae). Zoologischer Anzeiger, 295 23-33, https://doi.org/10.1016/j.jcz.2021.09.004.

Morrison C, Hero JM. 2003. Geographic variation in life-history characteristics of amphibians: a review. Journal of Animal Ecology, 72 (2), 270–279. doi:10.1046/j.1365-2656.2003.00696.x

Neta AFS, Silva MC, Ávila RW. 2018. Herpetofauna da Bacia Hidrográfica do Rio Salgado, Estado do Ceará, Nordeste do Brasil. Boletim do Museu de Biologia Mello Leitão, 40(1): 23-48.

Otero MA, Baraquet M, Pollo F, Grenat P, Salas N, Martino A. 2017a. Sexual size dimorphism in relation to age and growth in *Hypsiboas cordobae* (Anura: Hylidae) from Córdoba, Argentina. Herpetological Conservation and Biology, 12, 141–148.

Otero MA, Valetti JA, Bionda CL, Salas NE, Martino AL. 2017b. Are ploidy and age size-related? A comparative study on tetraploid *Pleurodema kriegi* and octoploid *P. cordobae* (Anura: Leptodactylidae) from Central Argentina. Zoologischer Anzeiger, 268, 136–142.

Paluh DJ, Stanley EL, Blackburn C. 2020. Evolution of hyperossification expands skull diversity in frogs. Proceedings of the National Academy of Sciences of the United States of America vol. 117, 15: 8554-8562.

Parmelee J. 1999. Trophic ecology of a tropical anuran assemblage. 11. 1-59.

Rebouças R, Silva HR, Sanuy D, Solé M. 2019. Sexual maturity and growth of male toads (*Rhinella ornata*): A comparison between insular and mainland populations, Zoologische Anzeiger, Volume 283, Pages 12-19, https://doi.org/10.1016/j.jcz.2019.07.002.

Roberto IJ, Ribeiro SC, Bezerra L, Carneiro PBM. 2011. Amphibia, Anura, Hylidae, *Trachycephalus atlas* Bokermann, 1966: Distribution extension and geographic distribution map. Check List, 7(3): 326-327.

Sanches PR, Santana MMS, Oliveira-Sousa AE, Costa-Campos CE. 2022. Sexual dimorphism in *Rhinella major* (Anura: Bufonidae) from eastern Brazilian Amazonia. NORTH-WESTERN JOURNAL OF ZOOLOGY 18 (2): 214-217.

Silva LA da, Carvalho PS, Pereira EA, Fadel R M, Dantas SP, Brandão RA, Santana DJ. 2020. Richness, diversity patterns, and taxonomic notes of amphibians from the Tocantins state. Biota Neotropica. Campinas: Revista Biota Neotropica, v. 20, n. 1, 22 p. Disponível em: <http://hdl.handle.net/11449/196542>.

Silveira AL, Pacheco SA. 2011. Um novo registro de *Trachycephalus mambaiensis* (Amphibia, Anura, Hylidae), no Estado de Minas Gerais, Brasil. Biotemas, 24 (3): 141-143, doi: 10.5007/2175-7925.2011v24n3p141.

Sinsch U. 2015. Review: Skeletochronological assessment of demographic life history traits in amphibians. Herpetological Journal, 25, 5–13.

Spradley MK, Jantz RL. 2011. Sex estimation in forensic anthropology: skull versus postcranial elements. Journal of forensic sciences, 56(2), 289–296. https://doi.org/10.1111/j.1556-4029.2010.01635.x

Trueb L. 1970. Evolutionary relationships of the casque-headed tree frogs with coossified skulls (Family Hylidae). University of Kansas Publications, Museum of Natural History, 18: 547–716.

Trueb L, Duellman WE. 1971. A synopsis of neotropical hylid frogs, genus *Osteocephalus*. Occas. Pap. Museum Nat. Hist. Univ. Kansas 1, 1–47.

Tschudi JJ. 1838. Classification der Batrachier mit Berücksichtigung der fossilen Thiere dieser Abtheilung der Reptilien. Neuchâtel: Petitpierre.

Vaz-Silva W, Maciel NM, Nomura F, Morais AR, Batista VG, Santos DL, Andrade SP, Oliveira AÂB, Brandão RA, Bastos RP. 2020. Guia de identificação das espécies de anfíbios (Anura e Gymnophiona) do estado de Goiás e do Distrito Federal, Brasil Central [online]. Curitiba: Sociedade Brasileira de Zoologia, 2020, 223 p. Zoologia: guias e manuais de identificação series. ISBN: 978-65-87590-01-1. https://doi.org/10.7476/9786587590011.

Wiens JJ. 2001. Character analysis in morphological phylogenetics: Problems and solutions. Systematic Biology, 50, 689–699.

Capítulo 1: External morphology and cranial diversity of casque-headed hylid frogs in the *Trachycephalus nigromaculatus* clade (Anura: Hylidae)

Abstract

Anuran morphology is crucial to understanding secondary sexual dimorphism and to species delimitation, due to its link with ecological variation within clades. Size variation affects the evolution of skull shape, and this variation can be studied through interspecific comparisons within the same developmental stage. Some anurans exhibit cranial hyperossification, with dermal layers fusing to cranial bones through exostosis, casquing, and co-ossification. The clade formed by *Trachycephalus nigromaculatus*, *T. atlas*, and *T. mambaiensis* comprises poorly studied casque-headed frogs with conservative external morphology that differ by subtle anatomic elements and hyperossification degrees of the skull. Using morphometrics measurements, geometric morphometrics and cranial osteology, we assessed the external morphology and the interspecific and intraspecific variation of cranial characteristics in *T. nigromaculatus*, *T. atlas*, *and T. mambaiensis.* LDA models presented interorbital distance, eye-nostril distance, and internasal distance the most discriminative variables between species. Female-biased sexual dimorphism was observed in body size in *T. nigromaculatus* and *T. atlas*; female-biased sexual dimorphism was also observed in head measurements and positive allometric relationships was found between body size and head measurements in the three species. The three-dimensional geometric morphometrics and skull anatomy improved the taxonomic identification of these species, where the skull morphology of *Trachycephalus mambaiensis* is considerably distinct from the other species. The detailed description of the skull of *Trachycephalus atlas* fills one of the gaps in the anatomy within the *Trachycephalus* genus. Further phylogenetic studies are warranted to elucidate intraspecific variation across the *Trachycephalus nigromaculatus* clade and support a detailed diagnosis for *T. nigromaculatus*, based on its redescription.

Keywords: Geometric morphometrics, head morphology, Lophyohylini, sexual dimorphism, skull, *Trachycephalus atlas*, *Trachycephalus mambaiensis*.

INTRODUCTION

Anuran morphology plays a crucial role in the characterization of secondary sexual dimorphism and species delimitation (Shine 1988, 1989, Wiens 2001, Lisle & Rowe 2013), given its close association with ecological variation within clades (Grizante et al. 2010, Muschick et al. 2012, Openshaw & Keogh 2014). Allometry emerges as a prominent factor in morphological variation (Klingenberg 2016), highlighting the correlation among traits resulting from size discrepancies (Huxley 1924, 1932). Different levels of size variation can be explored through integrated approaches, including investigations into interspecific size variations within a single ontogenetic stage, drawing from adult samples within a population (Drake and Klingenberg 2008; Weisensee and Jantz 2011; Freidline et al. 2015) or among closely related species (Ivanović et al., 2007). Even within a similar ontogenetic stage, body size varies considerably among organisms, influencing the evolution of skull shape (Callery & Elinson 2000).

Cranial osteology is generally considered evolutionarily conservative, playing a main role in the taxonomy of anuran species (Trueb 1973a). Frog skull anatomy is generally correlated with body size (Trueb & Alberch 1985), feeding biology (Emerson 1985), and microhabitat use (Trueb 1973, 1993). Some anurans present cranial hyperossification that is evidenced in dermal layers being fused to cranial bones by three levels of ossification, including the exostosis, which involves the formation of sculptured patterns (reticulate, pitting, or spiny patterns) through the appositional growth of dermal bone (Pombal et al. 2003, Buffrenil et al. 2016), the casquing, that involves the expansion of bones, forming helmet-like protuberances (Trueb 1970a), and the co-ossification, which involves the ossification of dermis between the skeleton (Trueb 1970a, 1973, Jared et al., 2005). The co-ossification is the maximum expression of hyperossification and is putatively related to phragmosis (Trueb 1970, 1973, 1993) and body-water balance in arid microhabitats (Andrade & Abe 1997, Navas et al., 2002).

Hylidae Rafinesque, 1815 is currently the richest Anura Family, comprising 438 species in Brazil (Frost 2024). The skull of hylids is generally marked by a tendency toward reduced ossification compared with other families (Trueb 1970a). However, the so-called “casque-headed frogs” in the Lophyohylini tribe often present extensive cranial ossification (Blotto et al. 2021). In the tribe, the species in the genus *Trachycephalus* present different degrees of skull hyperossification (Blotto et al. 2021). *Trachycephalus* contains 18 recognized species, mainly nocturnal explosive breeders, usually found calling perched in shrubs close to lentic water bodies (Rodrigues et al. 2005).

The clade formed by *Trachycephalus nigromaculatus* Tshudi, 1838, *T. atlas* Bokermann, 1966, and *T. mambaiensis* Cintra, Silva, Silva, Garcia, & Zaher, 2009 comprises poorly studied casque-headed frogs with conservative external morphology (Blotto et al. 2021). These species differ by subtle anatomy elements and hyperossification degrees of the skull (Bokermann 1966, Trueb 1970a, Cintra et al. 2009). In *Trachycephalus mambaiensis* frontoparietals not cover the prootics posteriorly and lacks a medial premaxillary notch (Cintra et al. 2009). *Trachycephalus atlas* differs from *T. nigromaculatus* by its longer than wide head, longer frontoparietal ridges, and by having a larger interorbital distance (Trueb 1970, Bokermann 1966). *Trachycephalus nigromaculatus* and T*. mambaiensis* differ from *T. atlas* by the presence of small or medium reddish spots sparsely disposed on the dorsum in life (Bokermann 1966, Cintra et al. 2009).

The distribution of this clade comprises the Atlantic Rain Forest, Caatinga, and Cerrado biomes. The *Trachycephalus nigromaculatus* range several environments, including the restinga phytophysiognomy within Atlantic Rainforest in the states of Espírito Santo (Almeida et al. 2011) and Rio de Janeiro (Lutz 1954), transitional areas of Atlantic Rainforest and Cerrado in state the of Bahia (Freitas & Lima 2009, Dias et al. 2010) and in forest fragments of Cerrado at the states of Minas Gerais, Goiás, and Piauí (Martins & Assalim 2019). All known records of *Trachycephalus atlas* are from Northeastern Brazil including enclaves of humid tropical forest, in the state of Pernambuco (Borges-Nojosa & Arzabe 2005); in the tropical dry forest of the states of Ceará (Roberto et al. 2011, Neta et al. 2018), Sergipe, Alagoas, and Paraíba (Magalhães et al. 2011) and in restinga habitats in the state of Bahia (Gondim-Silva et al. 2016). The few records of *Trachycephalus mambaiensis* are restricted to the Cerrado biome, including dry forests in the states of Minas Gerais (Silveira & Pacheco 2001, Dayrell et al. 2012), Goiás, (Vaz-Silva et.al. 2020), Tocantins (Silva et al. 2020), and Bahia (Freitas et al., 2011).

Considering the conservative external morphology of the species in the *Trachycephalus nigromaculatus* clade, we assessed the external morphology variation and the variation of skull characteristics in *T. nigromaculatus, T. atlas,* and *T. mambaiensis*.

MATERIALS AND METHODS

External morphology

We analyzed 125 specimens of *Trachycephalus nigromaculatus* (46 females and 79 males), 67 specimens of *T. atlas* (28 females and 39 males), and 24 specimens of *T. mambaiensis* (9 females and 15 males) housed in several Brazilian herpetological collections (see Appendix 1). We sexed the individuals based on the examination of gonads and secondary sexual characters (vocal sac, vocal slits, and nuptial pads). Individuals lacking secondary sexual characters and evident gonads were classified as juveniles.

We took 15 measurements (following Watters et al. 2016) from all individuals: snout-vent length (SVL), head length (HL), head width (HW), snout length (SL), internarial distance (ND), interorbital distance (IOD), eye diameter, measured horizontally (ED), eye−nostril distance, from the distal corner of orbit to proximal margin of the external nostril (EN), tympanum diameter, measured horizontally (TD), forearm length, from elbow to the proximal margin of the thenar tubercle (FAL), tibia length, (TL), thigh length, distance from the vent to the knee (THL), foot length, from the base of the inner metatarsal tubercle to the tip of Toe IV (FL), hand length, from the base of the outer palmar tubercle to the tip of Finger IV(HAL), and finger IV disk width, corresponding to the widest horizontal diameter of Finger IV (Fin4DW). We performed Linear Discriminant Analysis (LDA) (Venables & Ripley 2002) to summarize the morphometric differences between species. Boxplots were set up using three principal morphometric measurements. We tested differences in snout-vent length, head length, and head width among sexes using ANOVA.

Three-dimensional geometric morphometrics

We reconstructed and processed meshes from microCT scans of 33 crania of the three species (*T. nigromaculatus* = 19, *T. atlas* = 6, *T. mambaiensis* = 8). Meshes from microCT scans were created in Avizo Lite 9 and processed in 3D Slicer (Fedorov et al. 2012). One of us (IP) digitized a set of 20 landmarks on right side of the skull, using Morphodig v. 1.6.8, since our focus was not on the asymmetric component of shape (Larson 2004) (Fig. 1; for landmarks definitions see Table 1). A generalized Procrustes analysis was performed to align, rotate, and scale specimen landmark data to a common coordinate system and unit centroid size to remove variation in position, orientation, and size (Rohlf 1993). A Principal Component Analysis (PCA) using the covariance matrix of log-transformed measurements was performed on the average shape for all species. The differences in the shape described along the principal axis (PC) were summarized using wireframe graphs (Rohlf 1993; Adams et al. 2023). All analyses were performed using the MorphoJ software, version 1.08.01 (Rohlf 2010b, Klingenberg, 2011).

Cranial osteology

We cleared and stained (Taylor & Van Dyke, 1985) specimens of *Trachycephalus nigromaculatus* (n = 10)*, T. atlas* (n = 3), and *T. mambaiensis* (n = 2). Diaphanized specimens and meshes from microCT scans of crania were used for bone analyses and anatomical comparisons between species. The description of cranial osteology of *T. atlas* was performed following Duellman (1970) and Trueb (1970, 2006).

RESULTS

External morphology

The accuracy of the LDA model was 0.82, being interorbital distance ($p < 0.001$, F = 33.4), eye−nostril distance ($p < 0.001$, F = 34.5), and internasal distance ($p < 0.001$, F = 35.5) the variable with higher discrimination power (Fig. 2). Interorbital distance and eye-nostril distance were smaller in *Trachycephalus nigromaculatus* compared to *T. atlas* (Fig. 4). We found that females were larger in *Trachycephalus atlas* ($p < 0.001$, f = 26.4) and *T. nigromaculatus* ($p < 0.001$, f = 31.9). However, body length was not different for *T. mambaiensis* sexes (p = 0.1, f = 2.7). We detected differences in head length between sexes, with females exhibiting longer heads than males in *Trachycephalus atlas*, *T. nigromaculatus* ($p < 0.001$, f = 27.08), and *T. mambaiensis* ($p < 0.047$, f = 4.3). Furthermore, females exhibit wider heads in *Trachycephalus atlas* ($p < 0.001$, f = 27.7) and *T. nigromaculatus* ($p < 0.001$, f = 44.9), but not in *T. mambaiensis* ($p > 0.3$).

Trachycephalus mambaiensis is smaller than the other two species for the structures measured, except for its larger tympanum diameter and foot (metatarsal) lenght. The averages of the males' feet of *Trachycephalus nigromaculatus* and *T. atlas* were shorter than the females' feet of *T.* mambaiensis and the average of males' hands of *T. atlas* was shorter than the females' hands of *T. mambaiensis*, and finger IV disk width (Table 2). Head length (HL) and head width (HW) were not different between *T. nigromaculatus* and *T. atlas.*

We found positive allometric relationships between snout-vent length (SVL), head length, and head width in all species (Fig. 3), indicating that snout-vent length can predict head size in this clade. *Trachycephalus mambaiensis* exhibited a higher slope in head width (t = 0.83, R^2 = 0.79, F = 88.8, p<0.001) than *T. atlas* (t = 0.15, R^2 = 0.62, F = 111, p<0.001), and *T. nigromaculatus* (t <0.001, R^2 = 0.57, F = 164, p<0.001). We also observed a higher slope in *T. mambaiensis* on head length (t = 0.58, R^2 = 0.73, F = 64.05, p<0.001) than in *T. atlas* (t = 0.30, R^2 = 0.70; F = 155.60, p<0.001), and *T. nigromaculatus* (t = 0.01, R^2 = 0.61; F = 198.2, p<0.001). The higher slope observed in *Trachycephalus mambaiensis* indicates that the head tends to become proportionally smaller in larger individuals (Fig. 3), whereas in *T. atlas* and *T. nigromaculatus* the head becomes proportionally larger in larger individuals.

Three-dimensional geometric morphometrics

The first three PCs explained 69.6% of the total shape variation of the three-dimensional skull shapes in Principal Component Analysis (PCA). The PC1 captured 42.9% of the variation of the total skull shape variation (Fig. 4). Specimens with positive values along the PC1 axis showed an increase in skull width (landmark 6), a premaxilla wider than long (landmarks 1-2), the ramus of squamosal positioned in different levels and more distant to prootic (landmarks 7-8), a shorter nasal in its entire extension (landmarks 5,9,11), a shorter prootic and more close to squamosal (landmarks 17-18), a longer parasphenoid (landmarks 14-15) and a diminishing of size of frontoparietal (landmarks 12,19,20). In contrast, specimens with negative values presented a decrease in skull width (landmark 6), the ramus of squamosal positioned at same level, an enlargement of nasal at ventrolateral margin (landmarks 5,11), a longer prootic and covered by frontoparietal (landmarks 17-18), an enlargement in the size of frontoparietal (landmarks 12,19,20) and a diminishes in length of parasphenoid (landmarks 14-15) (Fig. 4).

Along the PC2 axis (Fig. 5), which explained 13,2% of the total shape variation, specimens with higher positive values showed an increase in cranial length (landmark 6), the arms of squamosal positioned closer to prootic (landmarks 7-8), an enlargement of nasal at ventrolateral margin (landmarks 5,11), and a lateral expansion of frontoparietal (landmarks 20), but not covering the prootic (landmark

18). In negative values of PC2, specimens presented a decrease in cranial length (landmark 6), the arms of squamosal positioned more distant to prootic (landmarks 7-8), a diminished nasal at the ventrolateral margin (landmarks 5,11), and a diminish of lateral expansion and extension of the posterior point of frontoparietal (landmarks 19-20).

The PC3 captured 8,3% of shape variation (Fig. 6), and specimens with positive values presented narrower skulls at the pars facialis of the maxilla level (landmark 3,4), a more vertical premaxilla (landmarks 1-3), longer squamosal which position more ventrally (lateral view), enlargement of nasal at the ventrolateral margin (landmarks 5,11), which decrease orbit size, decrease in parasphenoid width at level of lateral margin (landmarks 15,16), lateral extension of frontoparietal (landmark 20), that covered the prootic, and position of the posterior extension of frontoparietal (landmark 19) more proximate to medial line of skull.

Cranial osteology

Interspecific variation in cranial anatomy

The three species displayed distinct cranial hyperossification, expressed by the presence of exostosis, casquing, and co-ossification. Specimens of *Trachycephalus mambaiensis* (Fig. 10) have less hyperossification and specimens of *T. atlas* have the more extreme hyperossification (Fig. 8). Exostosis was expressed by a pitted and spiny dermal bone in skull of specimens of *Trachycephalus mambaiensis,* and by highly rugose and spiny dermal bones in skull of specimens of *T. nigromaculatus* and *T. atlas.* In the three species, the casquing was expressed by the expansion of frontoparietal, nasal, premaxilla, and squamosal, whereas integumentary-cranial co-ossification was observed in dermal sphenethmoid, squamosal, premaxilla, maxilla, and nasal. These features are readily observable on the dorsal surface of the head even without any anatomical preparation (Fig. 7).

We found interspecific variation between skull dermal elements of *Trachycephalus nigromaculatus*. *T. atlas*, and *T. mambaiensis.* Generally, the premaxilla of *Trachycephalus atlas* is more robust and the position of the alary process is larger vertically, being oriented dorso-posteriorly and thus more visible in ventral view (Fig. 8c). *Trachycephalus nigromaculatus* and *T. atlas* presented the zygomatic ramus of the squamosal significantly enlarged and forming a bony articulation with the posterior process of the maxilla. The squamosal of

Trachycephalus atlas is more extensive but presents the same shape in both ramus (Fig. 8), in contrast, the otic ramus of squamosal of *T. nigromaculatus* is more robust (Fig. 9). The frontoparietals of *Trachycephalus nigromaculatus* and *T. atlas* are attached to the exoccipital and bridges the crista parotica from the exoccipital to the squamosal (Fig. 8, Fig. 9). In contrast, the posterior margin of frontoparietals of *T. mambaiensis* terminates at level of semicircular channels (Fig. 10b). Different from *Trachycephalus nigromaculatus* and *T. atlas,* the alary processes of the premaxillaries of skull of specimens of *T. mambaiensis* does not articulate with the anterior tip of the nasal anterodorsally, the frontoparietal does not articulate with the anterior and posterior arms of the squamosal, and the frontoparietal do not present spinose processes (Fig. 10a, 10b). In dorsal view, the canthal ridge of *Trachycephalus mambaiensis* is wider (Fig. 10a, 10b) than other species. The occipital condyles of *Trachycephalus mambaiensis* are at the plane that joins the posterior borders of the quadratojugal (Fig. 10d), while it is located forward to the plane of the quadratojugal in *T. nigromaculatus* and *T. atlas* (Fig. 8c, Fig. 9g).

Intraspecific variation in cranial anatomy

We found intraspecific variation in skull dermal elements of *Trachycephalus nigromaculatus*. Some specimens presented frontoparietals that completely covered the prootic (Fig. 9a; n = 13), while others presented smaller lateral expansion of frontoparietals (Fig. 9b, 9c; n = 6). Some specimens presented no differences between zygomatic and otic ramus of the squamosal (Fig. 9b; n = 9), some presented a robust otic ramus of the squamosal compared to zygomatic (Fig. 9a, 9c; n = 9), some presented a ventral projection of the zygomatic ramus of the squamosal (Fig. 9f; n = 2) and others presented a thin and short squamosal, such as the squamosal observed in *T. mambaiensis* (Fig. 9e; n = 6). We do not find differences in the skull of *Trachycephalus atlas*, except for less exostosis in some specimens compared to others (Fig. 8a, 8b). The main variation in the skull dermal elements of *Trachycephalus mambaiensis* is in the shape of the frontoparietal bone (Fig 10a, 10b, 10c), which ventrally may (Fig. 10b, n=3; Fig. 10c, n = 4) or may not be attached (Fig. 10a; n= 1) to the exoccipital.

Description of *Trachycephalus atlas* cranium (wider as long, cranium length 26.90 mm; cranium width 26.04 mm). The description is based on the individual

MNRJ 19290, an adult female from the type-locality, in the Maracás municipality, state of Bahia (Fig. 8b, c, and d).

Maxillary arcade. The **premaxillaries** are robust and lie anteromedial to the maxillaries. The alary processes of the premaxillaries are greatly expanded and co-ossified anteriorly. Anterodorsally, the alary process does not articulate with the anterior tip of the nasal. The alary processes are concave posteriorly and are oriented approximately vertically. Dorsomedially, the alary process forms the anterior margin of the external naris. Ventrally, the lateral process articulates with the rostrum of maxilla. The *pars palatina* of the premaxillary is well developed and the posteromedial palatine process is conspicuous. The **maxillary** is moderately robust but lacks a labial flange. The *pars facialis* of the maxillary is well developed. It is the largest anterior to the orbit. Posterior to the external naris, the dorsal edge of the *pars facialis* is free and lies to the vomers. It articulates with the maxillary process of the nasal at the anterior margin of the orbit. The *pars facialis* increases in size to the anterior margin of the nasal and diminished to the orbit, but it is conspicuous along the entire length of the maxillary.

The *pars palatina* of the maxillary is well developed and extends from the anterior end of the bone posteriorly to the level of termination of the *pars dentalis*. Posteriorly, the maxillary firmly articulates with the quadratojugal which lies lateral adjacent to the maxillary. The labial surface of the maxillary is co-ossified and slightly rugose. There is an indistinct pattern of irregular bony ridges which radiate dorsally and anteriorly from the lower margin of the maxillary anterior to the orbit. Posterior and ventral to the orbit the labial surface of the maxillary is smooth, but the dorsal margin bears a series of small spines. The **septomaxilla** is a tiny, paired bone, encapsulated within the cartilages of the nasal capsule and thereby having no articulation with other bones. The **quadratojugal** increases in size posteriorly, whereas the maxillary diminishes in size. Posteriorly, the ossification of the quadratojugal invades the cartilage of the quadrate process.

Dermal investing bones. In the ventral view, the **vomer** lies lateral to the midline of the skull and ventral to the solum nasi and sphenethmoid. The paired vomers do not articulate medially and lies laterally to the midline of the skull and ventral to the solum nasi and sphenethmoid. The vomer is K-shaped, with the main axis formed by the anterior and posterior dentigerous processes, and laterally by the prechoanal and postchoanal processes. The post-choanal process is articulated with sphenethmoid. On the dorsal view, the lateral border of the main axis of the K forms a free projection that lies at vomer midpoint. The anterior end of the vomer lies dorsolateral to the premaxillary and converges medially just anterior to the prevomerine teeth. The dentigerous processes are slightly curved in a transverse plane. The prevomer bears well-developed lateral wings which form the anterior and medial margins of the internal naris. The **palatine** is a robust bone which lies posterior to the internal naris. The broad, distal end is lodged in the pars palatina of the maxillary and adjacent to the anterior maxillary process. The proximal end is pointed and lies ventral to the sphenethmoid and posterior to the prevomer. The palatine bears a series of odontoids along a prominent ventral ridge. The **nasals** are large. The anterior end of the nasal articulates with the dorsal margin of the alary process of the premaxillary. Laterally the nasal arches over the external nares and articulates ventrolaterally with the pars facialis of the maxillary at the corner of the orbit. The nasal forms the anterior margin of the orbit and articulates with the frontoparietal dorsolaterally. The canthal ridge is distinct. The ridge extends from the anterior end of the nasal along the lateral margin to the anterodorsal comer of the orbit. The entire surface of the nasal is involved in the integumentary-cranial co-ossification. Dorsally, near the orbit, the surface of the nasal is rugose. The rest of the nasal is marked by prominent bony ridges. The ridges are rough and form a radial pattern from the rugose area. The **frontoparietals** converge medially throughout their lengths. Anteriorly, the frontoparietal articulates with the nasal laterally and the dermal sphenethmoid medially. Anterolaterally, the frontoparietal forms a supraorbital shelf. Posterolaterally, the frontoparietal articulates with the otic ramus of the squamosal. Posteriorly, the frontoparietal terminates in spinose processes and there is an occipital crest. Ventrally, the frontoparietal is attached to the exoccipital; it bridges the crista parotica from the exoccipital to the squamosal. The entire dorsal surface of the frontoparietal is involved in integumentary-cranial co-ossification. Medially, the bone is rugose. From the central rugosity, irregular bony ridges radiate out toward the distal margins of the bone. The outer edges of the bone bear series of small spines. The most posterior margin is curved towards the dorsum and shows greater co-ossification. The **dermal sphenethmoid** is a triangular shaped bone, centrally located at the anterior level of the orbit; the bone lies posteromedial to the nasals and anteromedial to the frontoparietals. The dermal sphenethmoid is completely involved in integumentary-cranial co-ossification. The dorsal surface of the bone is rugose. The dorsally exposed dermal sphenethmoid is confluent with the underlying endochondral sphenethmoid. The margins of the orbitonasal foramen are bony. At the level of the foramen, the sphenethmoid is completely bony except for the distal tip of the anterolateral wing. Posteriorly, this tip expands distally to form a broad supraorbital shelf ventral to the nasal (Fig. 55). The cartilage diminishes in size and disappears posterior to the level of the frontoparietal-nasal articulation. In sections posterior to the dermal sphenethmoid, the roof of the endochondral sphenethmoid splits to form the frontoparietal fontanelle ventral to the frontoparietals.

Suspensorium. In dorsal view, the **squamosal** is a long bone which extends from the posterior edge of the orbit, along the posterolateral margin of the frontoparietal to a level posterior to the posterior edge of the frontoparietal. The dorsal and lateral surfaces of the squamosal are coossified and highly rugose and spiny. The anterior arm of the squamosal forms a part of tlie posterior margin of the orbit. Ventrally, the zygomatic ramus terminates dorsal to the maxillary; it is connected to the maxillary by connective tissue but does not articulate with the maxillary. The otic ramus of the squamosal is longer than the zygomatic; it lies at the posterior margin of the tympanum. The otic ramus articulates with the frontoparietal and crista parotica and extends posteriorly to these structures to the level of the posteroventral end of the ventral arm of the squamosal. The descendent ramus of the squamosal is moderately robust. Ventrally, it terminates between the quadratojugal laterally and the pterygoid medially, and dorsal to the quadrate process. The **pterygoid** is moderately robust; the anterior ramus lies adjacent to the posterior maxillary process. Posteriorly the pterygoid and pterygoid process diverge from the maxillary. The medial ramus is short and robust but does not articulate with the prootic medially. The posterior ramus is robust; it articulates with the quadrate process and descendent ramus of the squamosal posteriorly. The **quadratojugal** is well developed. The anterior end lies medially adjacent to the maxillary at the level of the optic foramen.

Endocranial braincase. The endocranial braincase is complete, consisting of sphenethmoid, prootics, and exoccipitals, which are partially covered by the frontoparietals dorsally and the parasphenoid ventrally. The sphenethmoid forms the floor, anterolateral walls, and the edges of the roof of the braincase. It is ossified and it is often in contact with the optic foramen. It is dorsally visible between the nasals and frontoparietals. The lateral-posterior margins are convex. Dorsally the sphenetmoid overlaps with the posterior 1/3 of the nasals; ventrally it overlaps with

1/2 of the palatines, the anterior 2/3 of the frontoparietals, and vomers. An orbitonasal foramen is visible, anterolaterally, and is enclosed by the sphenethmoid. The prootics are fused with the exoccipitals, forming the posterior region of the braincase and each one contributes to the otic capsules. The posterior 2/3 of prootics is fused with squamosal. They lack dorsal ornamentation. Anteriorly, there is a large ovoid prootic foramen, totally enclosed by bone. The **exoccipitals** form the posteromedial walls of the otic capsules, the margins of the foramen magnum and the occipital condyle. They are ventrally covered by the parasphenoid. The occipital condyles are protuberant, separated, divergent to upward and semiovoid-shaped. They are located forward in relation to the plane that joins the posterior borders of the quadratojugal. The jugular foramen is lateral to the occipital condyles, entering the posterior wall of the otic capsule.

DISCUSSION

External morphology

Morphometric measurements can serve as a tool for discrimination of species of *Trachycephalus nigromaculatus* clade, where most morphometric averages are smaller in *T. mambaiensis* (Table 2). Previously, it was observed that the larger interorbital distance and longer head length in *Trachycephalus atlas* differentiate it from *T. nigromaculatus* (Bokermann 1966, Trueb 1970). Our observations suggest that head length is not a reliable feature for discrimination between *Trachycephalus atlas and T. nigromaculatus*, and the differences extend beyond interorbital distance, with eye-nostril and internasal distances also aiding in species differentiation. Variation in interorbital distance significantly influences eye position, likely reflecting activity patterns of anurans (Jiang et al. 2022). Species with greater foraging mobility exhibit larger interorbital distances compared to those with slower foraging mobility (Thomas et al 2020, Jiang et al. 2022).

We observed female-biased sexual dimorphism in body size in *Trachycephalus nigromaculatus* and *T. atlas* but not in *T. mambaiensis.* Sexual dimorphism in body size is widespread among numerous anuran species, with females typically being larger than males (Shine 1989, Nali et al., 2014). This phenomenon is often linked to the greater reproductive investment of females, which is characterized by increased egg production. As a result, larger female body sizes are favored to accommodate larger clutch sizes (Gibbons & McCarthy 1983).

Conversely, mate selection in anurans is significantly shaped by male-male competition for access to females, particularly in some explosive breeding species (Dittrich & Rodel 2023). This competitive interaction frequently leads to the preferential choice of larger males, as they hold competitive advantages in securing mating opportunities (Kupfer 2007). Although larger male size may be advantageous in intrasexual contests (male-male competition), male frogs also rely on other fitness-related traits besides body size, such as forearm thickness for male displacement, energy expenditure in calling activity, or early sexual maturity (e.g., Howard and Kluge 1985, Howard et al. 1994); thus, some species can show less-pronounced SSD (Nali et al. 2014). Sexual dimorphism in size remains uncertain whether *T. mambaiensis* since both sexes may encounter selective pressures favoring larger body sizes and any discernible size difference could be subtle and inadequately represented in our limited sample.

Sexual dimorphism was also observed in head measurements of the three species, in which females' heads were larger and wider. In the *Leptodactylus* genus and salamander species, males commonly display wider and longer heads in comparison to females (Bovero et al. 2003, Hayek & Heyer 2001). When sexual dimorphism is predominantly manifested in head dimensions rather than body size, discerning the influences of sexual and natural selection is challenging (Shine 1989). Furthermore, the widespread prevalence of head dimorphism across various genera may suggest a phylogenetic autocorrelation (Abouheif & Fairbairn 1997). This autocorrelation was corroborated by our allometric analyses, in which head measurements are not an independent feature and *Trachycephalus nigromaculatus,* and *T. atlas* exhibited isometric growth, indicating that larger body sizes tend to exhibit larger head measurements.

Three-dimensional geometric morphometrics

Our first-ever reference to three-dimensional geometric morphometrics for the *Trachycephalus* genus helped reveal fine-scale differences in skull shape and has proven effective as a supportive tool in the osteological description and comparison of *Trachycephalus nigromaculatus, T. atlas*, and *T. mambaiensis.* In terms of shape, specimens of *Trachycephalus mambaiensis* appear distinctly separate from the other species, such as in morphometric measurements, where the species is smaller. *Trachycephalus mambaiensis* presents an increase in skull width, premaxillae wider than long, squamosal processes at different levels, which otic ramus positioned more dorsally, nasals shortened in its margins, shorter prootics, longer parasphenoid and a reduced frontoparietal, while *T. nigromaculatus* and *T. atlas* present a decrease in skull width, longer squamosal, nasal and prootic, shorter parasphenoid and larger frontoparietals. Even in PC2, all specimens of *Trachycephalus atlas* remain clustered together with *T. nigromaculatus*. However, PC3 allowed the distinction between *Trachycephalus nigromaculatus* and *T. atlas*, where specimens of *T. atlas* present, in positive values, a narrower skull at the pars facialis of the maxilla level, verticalization of premaxilla, arms of squamosal at same levels, enlargement of nasal at ventrolateral margin, and position of the posterior extension of frontoparietal more proximate to medial line of skull. Considering the low similarity observed in skull shape between *Trachycephalus nigromaculatus* and *T. mambaiensis* (except for the smaller size of the squamosal in some *T. nigromaculatus* specimens, n = 6), one of the *T. nigromaculatus* skulls was positioned within the confidence ellipse of *T. mambaiensis*, reflecting the species misidentification in its original collection (Voucher UFV 11714). Incorrect identifications may arise due to the co-occurrence of these species in the states of Minas Gerais and Bahia (Silveira & Pacheco 2001, Freitas et al. 2011, Dayrell et al. 2012, Martins & Assalim 2019), coupled with the potential for larger individuals of *Trachycephalus mambaiensis* to exhibit pronounced cranial hyperossification.

Cranial osteology

The three species of *Trachycephalus nigromaculatus* clade displayed exostosis, casquing, and co-ossification, which varies the hyperossification degree observed in the skull between species and specimens. Duméril & Bibron (1841) previously noted that the degree of co-ossification in *T. nigromaculatus* may increase with age, likely turning bone sutures indistinguishable in older individuals. Although we did not specifically test the relationship between age and increased co-ossification, we agree with the previous suggestions of Duméril & Bibron (1941), and we found that hyperossification could be potentially linked to changes in the *Trachycephalus* cranial morphology throughout its growing (Alberch et al. 1979, Reilly et al. 1997). Some specimens of *Trachycephalus mambaiensis* with a less hyperossified skull and faint reddish spots on the dorsum may even be confused with *T. typhonius* (Linnaeus 1758) (*pers. obs.*) by those who are poorly familiarized with these species.

The casquing expressed in these species by expanded frontoparietal and nasal regions suggests that this condition may mitigate evaporative water loss, potentially due to the pronounced moisture gradient between ground and canopy levels in tropical rainforests (Scheffers et al. 2013).

The use of restinga bromeliads as retreat sites are known for *Trachycephalus nigromaculatus*, while *T. atlas*, which occurs mainly in arid environments in northeast Brazil, also utilizes bromeliads as retreat sites. Although the relationship between these frogs and the use of bromeliads deserves further study, phragmosis combined with the expanded and hyperossified skull roof allows these frogs to retract their eyes beneath the bony shelves, protecting them against predators (Paluh et al. 2020), and avoid further evaporative water loss (Andrade & Abe 1997, Navas et al. 2002). We have no information regarding diurnal retreat sites for *T. mambaiensis*. However, since bromeliads are uncommon where the species occurs, we suggest that *T. mambaiensis* utilize tree holes and log crevices as shelter and protection, likely presenting phragmotic behavior using its cranium as bony shelve.

Analyses of skull anatomy of *Trachycephalus nigromaculatus, T. atlas,* and *T. mambaiensis* reveal intraspecific and interspecific variations, that can improve the taxonomic identification of these species. The skull morphology of *Trachycephalus mambaiensis* is considerably distinct from the other species, especially by presenting a lower degree hyperossification, a cranium wider than long, the position of occipital condyle at the same level of posterior borders of the quadratojugal, smaller size of the squamosal, the prootic, and the parasphenoid, as well as the small size and the distinctive shape of the frontoparietal. *Trachycephalus atlas* can be distinguished by *T. nigromaculatus* mainly by the squamosal largest extension and position, having the same shape in both rami, the largest size of premaxilla and the position of the alary process of the premaxilla, which is more vertically oriented, and by the frontoparietal shape. The zygomatic ramus of the squamosal is enlarged, forming a bony articulation with the posterior process of the maxilla present in some *Trachycephalus nigromaculatus* and in specimens *T. atlas* is a feature commonly found in hyperossified vertebrate predators (Paluh et al. 2020), in which the contact between the squamosal and the maxilla enlarges the adductor chamber of the jaw adductor muscles, associated with bite force (Emerson 1985).

CONCLUSION

Additional morphological parameters such as eye-nostril and internasal distances contribute to species differentiation. Sexual dimorphism, especially in body size and head measurements, was evident in *Trachycephalus nigromaculatus*, *T. atlas,* and *T. mambaiensis*, underscoring the influence of reproductive investment and mate selection dynamics. Geometric morphometric analysis revealed significant skull shape variations among species, with *Trachycephalus mambaiensis* exhibiting significative distinct cranial characteristics compared to the other species studied. The degree of hyperossification observed in some specimens emphasizes the potential morphological changes throughout an individuals' development in these species. Similar to *Trachycephalus* nigromaculatus and *T. atlas*, *T. mambaiensis* may display phragmotic behavior associated with tree holes and log crevices, with ecological functions related to protection and water conservation. The detailed description of the skull of *Trachycephalus atlas* fills one of the gaps in the anatomy within the *Trachycephalus* genus. Further phylogenetic studies are warranted to elucidate intraspecific variation across the *Trachycephalus nigromaculatus* clade and support a detailed diagnosis for *T. nigromaculatus*, based on its redescription.

Literature cited

Andrade DV., Abe AS. 1997. Evaporative water loss and oxygen uptake in two casque-headed tree frogs, *Aparasphenodon brunoi* and *Corythomantis greeningi* (Anura, Hylidae). Comp. Biochem. Physiol. A 118A, 685–689.

Barros FC., Herrel A., Kohlsdorf T. 2011. Head shape evolution in Gymnophthalmidae: Does habitat use constrain the evolution of cranial design in fossorial lizards?J. Evol.Biol.24, 2423–2433.

Blotto BL, Lyra ML., Cardoso MC., Trefaut Rodrigues M, Día R.I., Marciano-Jr E., Dal Vechio F., Orrico VG., Brandão RA., Lopes de Assis C., Lantyer-Silva AS., Rutherford MG., Gagliardi-Urrutia G., Solé M., Baldo D., Nunes I., Cajade R., Torres A., Grant T., Jungfer K.-H., da Silva HR., Haddad CFBH., Faivovich J. 2021. The phylogeny of the Casque-headed Treefrogs (Hylidae: Hylinae: Lophyohylini). Cladistics, 37: 36-72.

Bokermann WCA. 1966. Una nueva especie de *Trachycephalus* de Bahia, Brasil (Amphibia, Hylidae). Neotropica. La Plata 12: 120–124.

Callery EM., Elinson RP. 2000. Thyroid hormone-dependent metamorphosis in a direct developing frog. Proc. Natl Acad. Sci. USA 97, 2615–2620.

Cintra CED., Silva HLR., Silva NJ., Garcia Jr PC. de A., Zaher H. 2009. A new species of *Trachycephalus* (Amphibia, Anura, Hylidae) from the state of Goiás, Brazil. Zootaxa 1975: 58–68.

Duellman WE. 1970. The Hylid Frogs of Middle America. 2 volumes. Monograph. Museum of Natural History, University of Kansas: 1–753.

Drake A, Klingenberg C. 2007. The pace of morphological change: historical transformation of skull shape in St Bernard dogs. Biological sciences / The Royal Society. 275. 71-6. 10.1098/rspb.2007.1169.

Emerson S.B. 1985. Skull shape in frogs - Correlations with diet. Herpetologica1985, 177–188.

Faivovich J., Pereyra MO., Celeste Luna M., Andreas H., Blotto BL., Vasquez-Almazan CR., McCranie JR., Sanchez DA., Baeta D., Araujo-Vieira K., Koehler G., Kubicki B., Campbell JA, Frost DR., Wheeler WC., Haddad CFBH. 2018. On the monophyly and relationships of several genera of Hylini (Anura: Hylidae: Hylinae), with comments on recent taxonomic changes in Hylids. South American Journal of Herpetology, 13: 1–32.

Fedorov A., Beichel R., Kalpathy-Cramer J., Finet J., Fillion-Robin J-C., Pujol S., Bauer C., Jennings D., Fennessy F.M., Sonka M., Buatti J., Aylward SR., Miller JV., Pieper S., Kikinis R. 2012. 3D Slicer as an Image Computing Platform for the Quantitative Imaging Network. Magnetic Resonance Imaging. Nov;30(9):1323-41.

Frost DR. Amphibian Species of the World: An Online Reference. Version 5.5 (April, 2024). Electronic Database on https://amphibiansoftheworld.amnh.org/.

Gibbons MM, McCarthy TK. 1983. Age determination of frogs and toads (Amphibia, Anura) from Northwestern Europe. Zoologica Scripta, 12, (2), 145–151.

Hayek LAC, Heyer WR, Gascon C. 2001. Frog morphometries: a cautionary tale. Alytes. Retrieved from http://vertebrates.si.edu/herps/herps_pdfs/heyer_pdfs/2000s/Hayek_Heyer_Gascon_2001_18_153 -177.PDF

Huxley J. 1924. Applied biology. Rice Institute Pamphlet-Rice University Studies, 11(4).

Huxley JS. 1932. Problems of Relative Growth. The Johns Hopkins University Press, Baltimore.

Ivanović A, Vukov TD, Džukić G, Tomaševič N, Kalezić ML. 2007. Ontogeny of skull size and shape changes within a framework of biphasic lifestyle: a case study in six Triturus species (Amphibia, Salamandridae). Zoomorphology 126: 173–183.

Jiang Y., Chen C., Liao W. 2022. Anuran interorbital distance variation: the role of ecological and behavioral factors. Integrative Zoology 2022; 0: 1–10.

Klingenberg CP. 2011. MorphoJ: An Integrated Software Package for Geometric Morphometrics. Molecular Ecology Resources, 11, 353-357.

http://dx.doi.org/10.1111/j.1755-0998.2010.02924.x

Klingenberg CP., Duttke S., Whelan S., Kim M. 2016. Developmental plasticity, morphological variation and evolvability: a multilevel analysis of morphometric integration in the shape of compound leaves. J Evol Biol 25:115–129

Larson PM. 2004. Chondrocranial morphology and ontogenetic allometry in larval *Bufo americanus* (Anura, Bufonidae). Zoomorphology; 123: 95–106

Lisle SPD, Rowe, L. 2013. Correlated evolution of allometry and sexual dimorphism across higher taxa. The America Naturalist 182: 630-639.

Navas CA., Jared C. Antoniazzi MM. 2002. Water economy in the casque-headed tree-frog *Corythomantis greening* (Hylidae): Role of behaviour, skin, and skull skin co-ossification. J. Zool. (Lond.)257, 525–532.

Paluh DJ., Stanle, EL., Blackburn DC. 2020. Evolution of hyperossification expands skull diversity in frogs. *Proceedings of the National Academy of Sciences of the United States of America* vol. 117, 15: 8554-8562.

Reilly SM., Wiley EO., Meinhardt DJ. 1997. An integrative approach to heterochrony: The distinction between interspecific and intraspecific phenomena. Biol. J. Linn. Soc.Lond.60, 119–143.

Rohlf FJ. 1993. Relative-warp analysis and an example of its application to mosquito wings. In: Marcus L.F., Bello E. Garcia-Valdecasas A. (Eds.), Contributions to Morphometrics. Museo Nacional de Ciencias Naturales, Madrid; 131–159.

Rohlf J. 2010b. TpsRelw program version 2.16. Ecology and evolution, SUNY at Stony Brook.

RStudio Team. 2023. RStudio: Integrated Development for R. RStudio, PBC, Boston, MA URL http://www.rstudio.com/.

Scheffers B., Phillips B., Laurance W., Sodhi N., Diesmos A. Stephen W. 2013. Increasing arboreality with altitude: A novel biogeographic dimension. Proceedings. Biological sciences / The Royal Society. 280. 20131581. 10.1098/rspb.2013.1581.

Sheil CA., Alamillo H. 2005. Osteology and skeletal development of *Phyllomedusa vaillanti* (Anura: Hylidae: Phyllomedusinae) and a comparison of this arboreal species with a terrestrial member of the genus. J Morphol. Sep;265(3):343-68. doi: 10.1002/jmor.10362.

Shine R. 1988. The evolution of large body size in females: a critique of Darwin’s ‘‘fecundity advantage’’ model. The American Naturalist 131: 124–131.

Shine R. 1989: Ecological causes for the evolution of sexual dimorphism: a review of the evidence. Quarterly Review of Biology 64: 419–461.

Taylor WR, Van Dyke GC. 1985. Revised procedures for staining and clearing small fishes and other vertebrates for bone and cartilage study. Cybium, 9, 290–300.

Thomas KN, Gower DJ., Bell RC., Fujita MK., Schott RK., Streicher JW. 2020. Eye size and investment in frogs and toadscorrelate with adult habitat, activity patternand breeding ecology.Proc. R. Soc. B287:20201393.http://dx.doi.org/10.1098/rspb.2020.1393

Trueb L., Alberch, P. 1985. “*Miniaturization and the anuran skull: A case study of heterochrony*” in Functional Morphology in Vertebrates, H. R. Duncker, G. Fleischer, Eds. (Gustav Fischer Verlag, 1985), pp. 113–121.

Trueb L. 1970. Evolutionary relationships of the casque-headed tree frogs with coossified skulls (Family Hylidae). University of Kansas Publications, Museum of Natural History, 18: 547–716.

Trueb L, Duellman WE. 1971. A synopsis of neotropica hylid frogs, genus *Osteocephalus*. Occas. Pap. Museum Nat. Hist. Univ. Kansas 1, 1–47.

Trueb L. 1973. Bones, frogs, and evolution. In: Vial, J.L. (Ed.). Evolutionary Biology of the Anurans. University of Missouri Press, Columbia. p. 65-135.

Trueb L. 2006. Evolution of the Amphibian Skull. Copeia, Lawrence Ed. 3, (Sep 15, 2006): 578- 579.
Tschudi JJ. (1838). Classification der Batrachier mit Berücksichtigung der fossilen Thiere dieser Abtheilung der Reptilien. Neuchâtel: Petitpierre.

Watters JL, Cummings ST, Flanagan RL, Siler CD. 2016. Review of morphometric measurements used in anuran species descriptions and recommendations for a standardized approach. Zootaxa 4072 (4): 477–495.

Wiens JJ. 2001. Character analysis in morphological phylogenetics: Problems and solutions. Systematic Biology, 50, 689–699.

Table 1. Description of landmarks digitized on 3D analysis of species of *T. nigromaculatus* group.

Landmark	Description
1,2,3,4	anteromedial point of premaxilla, anterodorsal point of premaxilla, anterolateral point of premaxilla, anteroventral point of maxilla
5	posterolateral point of the nasal
6	most posterior end of quadratojugal
7,8	distal point of the otic ramus of squamosal, distal point of the zygomatic ramus of squamosal
9	most anterior point of nasal
10	most anterior point of the tectum nasi
11	nasal-frontoparietal joint at lateral margin
12	posteromedial margin of the frontoparietal
13	most caudal point of the skull
14,15,16	posterior end of the parasphenoid, lateral end in the ala of the parasphenoid, anterior point of the parasphenoid
17,18	posteromedial end of prootic, anteromedial end of prootic
19,20	points in frontoparietal

Table 2. Morphological measurements (mm) of *Trachycephalus nigromaculatus* clade. Values are presented as mean ± SD (range). Abbreviations: SVL, snout-vent length; HL, head length, HW, head width; SL, snout length; IND, internarial distance; IOD, interorbital distance; ED, eye diameter; END, eye−nostril distance; TD, tympanum diameter; FAL, forearm length; TL, tibia length; THL, thigh length; FL, foot length; Fin4DW, finger IV disk width.

	T. nigromaculatus Females (n=46)	*T. nigromaculatus* Males (n=79)	*T. atlas* Females (n=28)	*T. atlas* Males (n=39)	*T. mambaiensis* Females (n=9)	*T. mambaiensis* Males (n=15)
SVL	89.2±7.5 (72.9–104.9)	82.8±6.0 (65.9–96.5)	88.5± 5.2 (76.8–100.7)	82.0±5.2 (64.2–93.7)	80.9±9.3 (77.1–94.2)	75.6±7.0 (64.4–88.9)
HL	26.1±1.8 (21.9–30.1)	24.4±1.6 (20.2–28.5)	25.8±1.6 (20.4–28.5)	24.3±1.5 (21.1–28.2)	22.7±1.9 (19.7–25.9)	21.3±1.4 (19.0–24.4)
HW	28.8±2.5 (22.9–33.2)	26.3±1.7 (22.3–30.6)	28.5±1.5 (23.4–31.0)	26.3±1.7 (22.3–31.2)	25.4±2.6 (20.5–29.5)	23.6±1.7 (20.3–27.3)
SL	12.7±1.3 (9.8–17.8)	11.8±0.9 (8.6–14.0)	13.0±1.0 (9.8–14.6)	12.2±0.8 (10.0–13.9)	10.6±1.2 (8.7–12.7)	10.4±0.6 (9.3–11.2)
IND	6.4±0.6 (5.1–8.0)	5.9±0.4 (5.0–6.7)	6.2±0.5 (4.8–6.9)	5.9±0.5 (4.8–6.9)	5.3± 0.6 (4.6–6.9)	4.9±0.4 (4.5–5.8)

IOD	12.8±1.2 (9.8–15.1)	11.5±1.0 (8.6–13.8)	13.8±1.4 (10.6–16.1)	12.6±1.0 (10.0–14.3)	9.7±1.4 (7.9–12.1)	9.3±0.8 (7.9–11.2)
ED	7.6±0.8 (5.6–9.4)	7.1±0.7 (3.6–8.5)	7.5±0.6 (6.4–9.1)	7.1±0.5 (6.3–8.5)	6.8±0.5 (6.0–7.6)	6.3±0.6 (5.4–7.3)
END	7.7± 0.8 (6.4–9.3)	7.0±0.6 (5.6–8.5)	8.3±0.9 (5.6–9.4)	7.7±0.7 (5.9–9.3)	6.4±1.1 (5.5–8.6)	6.3±0.5 (5.6–7.3)
TD	5.3±0.5 (4.2–6.2)	4.9±0.3 (4.0–5.6)	5.1±0.3 (4.2–5.8)	4.9±0.3 (4.1–5.7)	5.0±0.4 (4.5–5.5)	4.7±0.4 (4.2–5.6)
FAL	13.9±1.4 (10.9–16.8)	12.7±1.1 (10.4–15.4)	13.4± 1.0 (11.0–15.5)	12.2±1.2 (10.2–14.8)	13.2±1.6 (10.8–15.6)	11.6±1.3 (9.3–13.9)
TL	40.9±3.2 (34.0–45.9)	37.6±2.2 (32.1–41.8)	40.1±2.3 (32.0–43.3)	37.4±2.0 (33.2–42.5)	37.5±4.2 (30.3–44.2)	34.4±2.7 (29.2–40.1)
THL	39.1±3.9 (30.8–45.6)	36.0±3.0 (26.2–41.8)	39.2±2.6 (31.1–42.8)	36.7±2.6 (24.2–40.7)	36.1±5.0 (29.6–44.0)	32.8±3.7 (23.4–39.4)
FL	35.3±3.0 (28.8–40.9)	32.7±2.6 (25.8–39.2)	34.0±2.2 (27.1–37.7)	32.1±2.2 (27.6–39.0)	32.2±3.7 (26.3–39.8)	29.4±2.9 (23.5–36.4)
HAL	26.9±2.1 (22.3–30.5)	25.3±2.7 (19.2–36.5)	25.9±2.0 (19.8–29.4)	24.5±1.6 (20.5–29.4)	24.8±3.1 (19.1–30.7)	22.7±2.2 (17.9–28.3)

Fin4DW	4.9±0.6 (3.3–6.0)	4.5±0.6 (3.0–5.9)	4.4±0.6 (3.0–5.8)	4.3±0.6 (2.5–5.6)	4.3±0.8 (3.0–5.7)	4.0±0.6 (2.9–5.4)

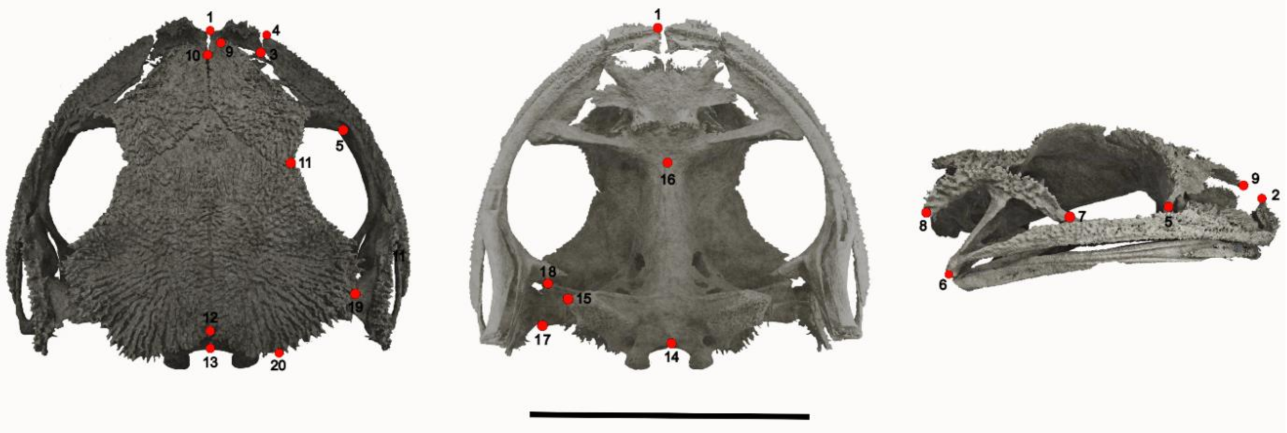

Figure 1. Schematic imaging showing the position of landmarks (red dots) digitized on the dorsal, ventral, and lateral view of the skull of species of the *Trachycephalus nigromaculatus* clade.

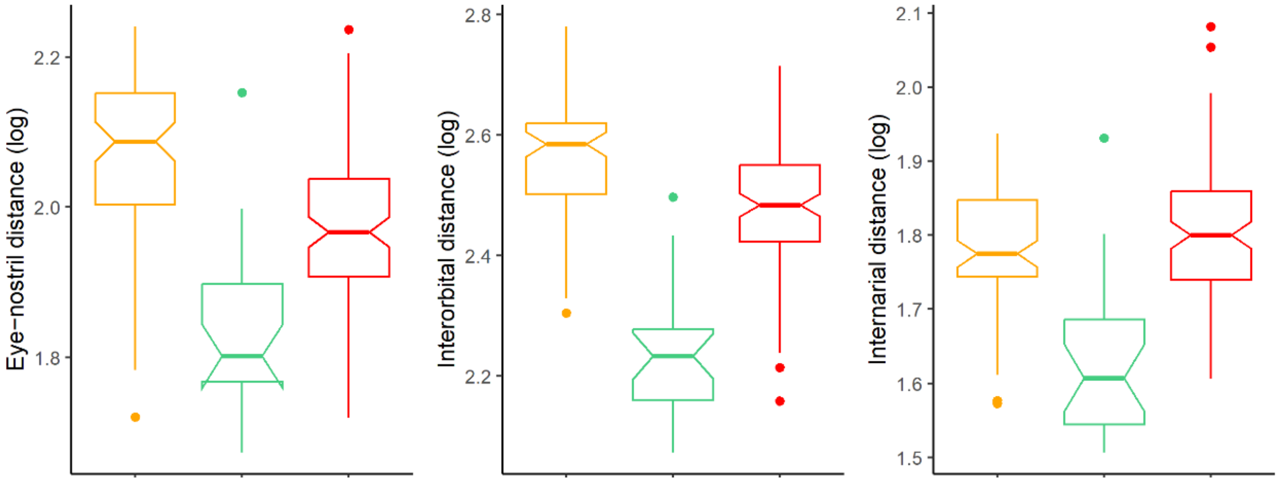

Figure 2. Variables with higher discrimination power by Linear Discriminant Analyses (LDA) in the three species of *Trachycephalus* - *T. atlas* (yellow), *T. mambaiensis* (greenish blue), and *T. nigromaculatus* (red).

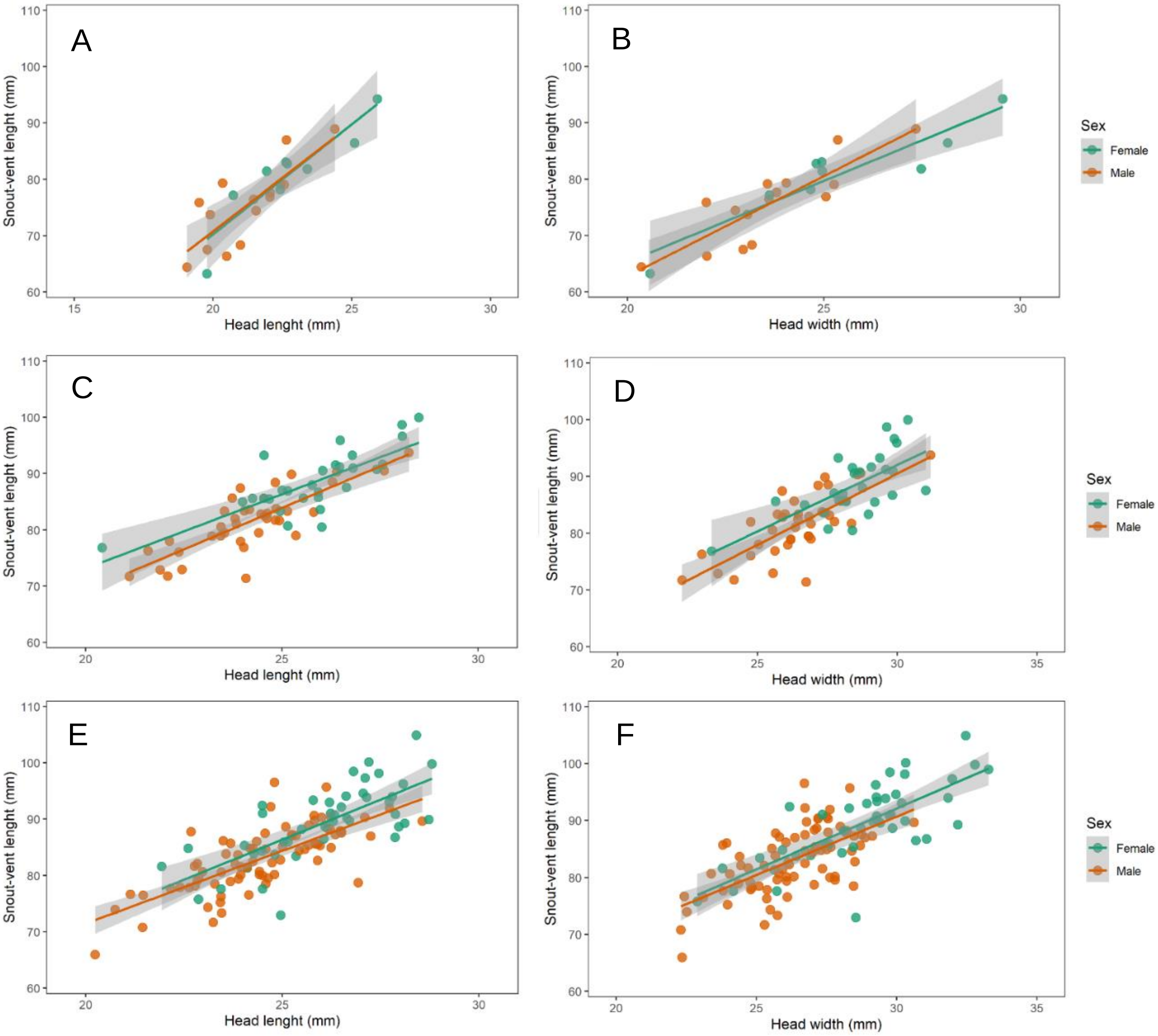

Figure 3. Body-head allometry of the three species of *Trachycephalus.* (a) Head length of *T. mambaiensis* and (b) head width. (c) Head length of *T. atlas* and (d) head width. (e) Head length of *T. nigromaculatus* and (f) head width.

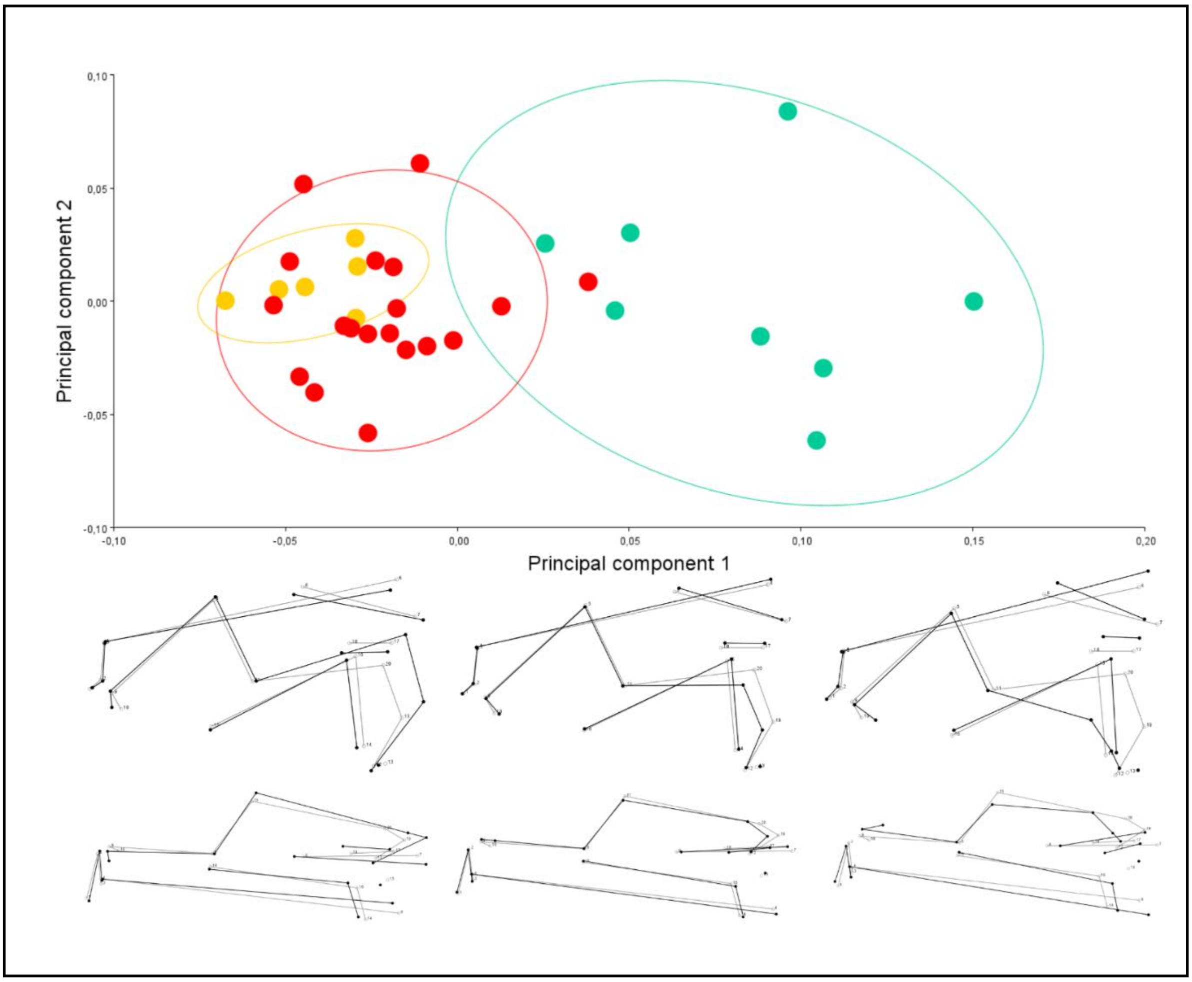

Figure 4. Morphospace formed by PC1 and PC2 considering the overall shape in the three species of *Trachycephalus - T. nigromaculatus* (red), *T. atlas* (yellow), *T. mambaiensis* (greenish blue). Black lines represent the target and grey lines the mean shape.

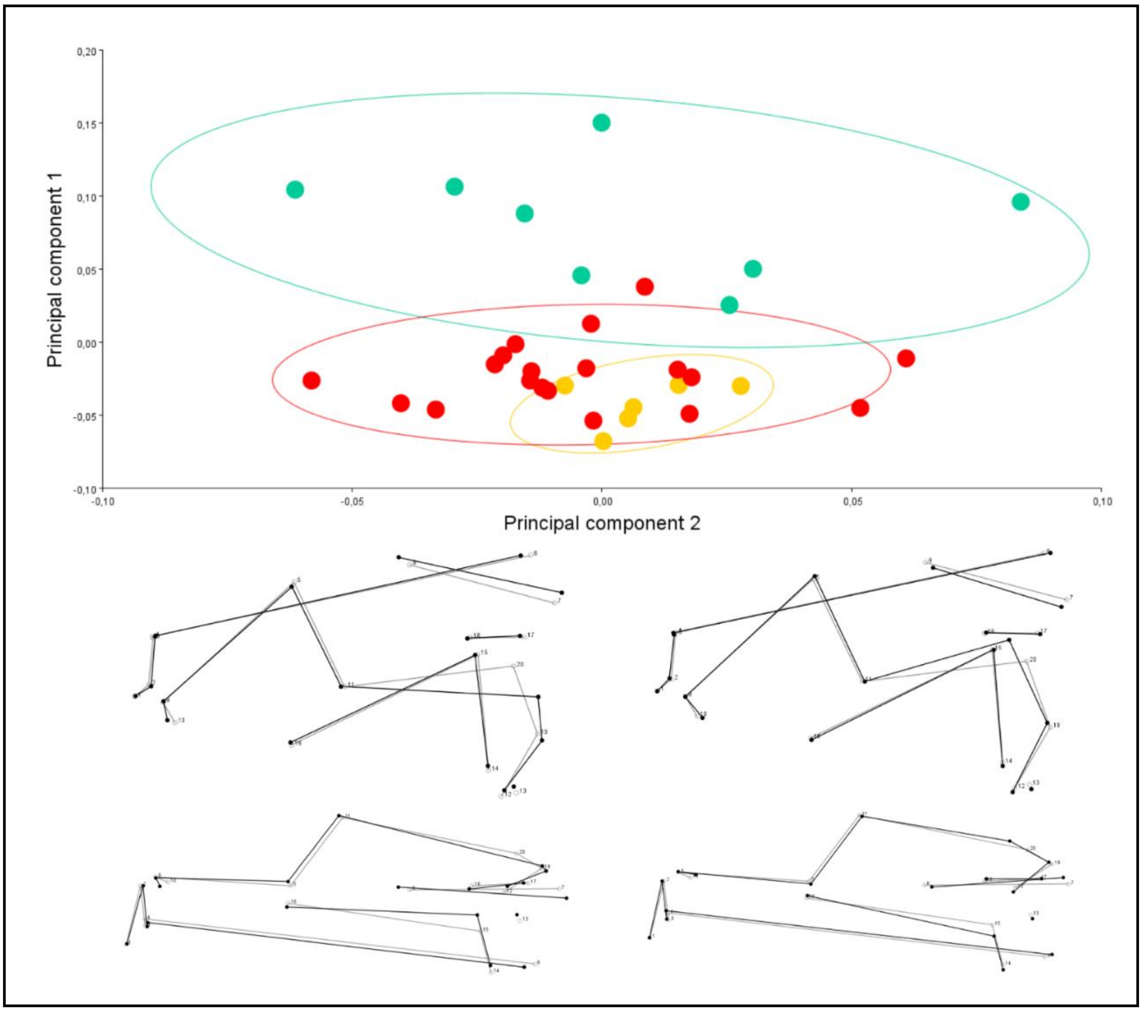

Figure 5. Morphospace formed by PC2 and PC1 considering the overall shape in the three species of *Trachycephalus* - *T. nigromaculatus* (red), *T. atlas* (yellow), *T. mambaiensis* (greenish blue). Black lines represent the target and grey lines the mean shape.

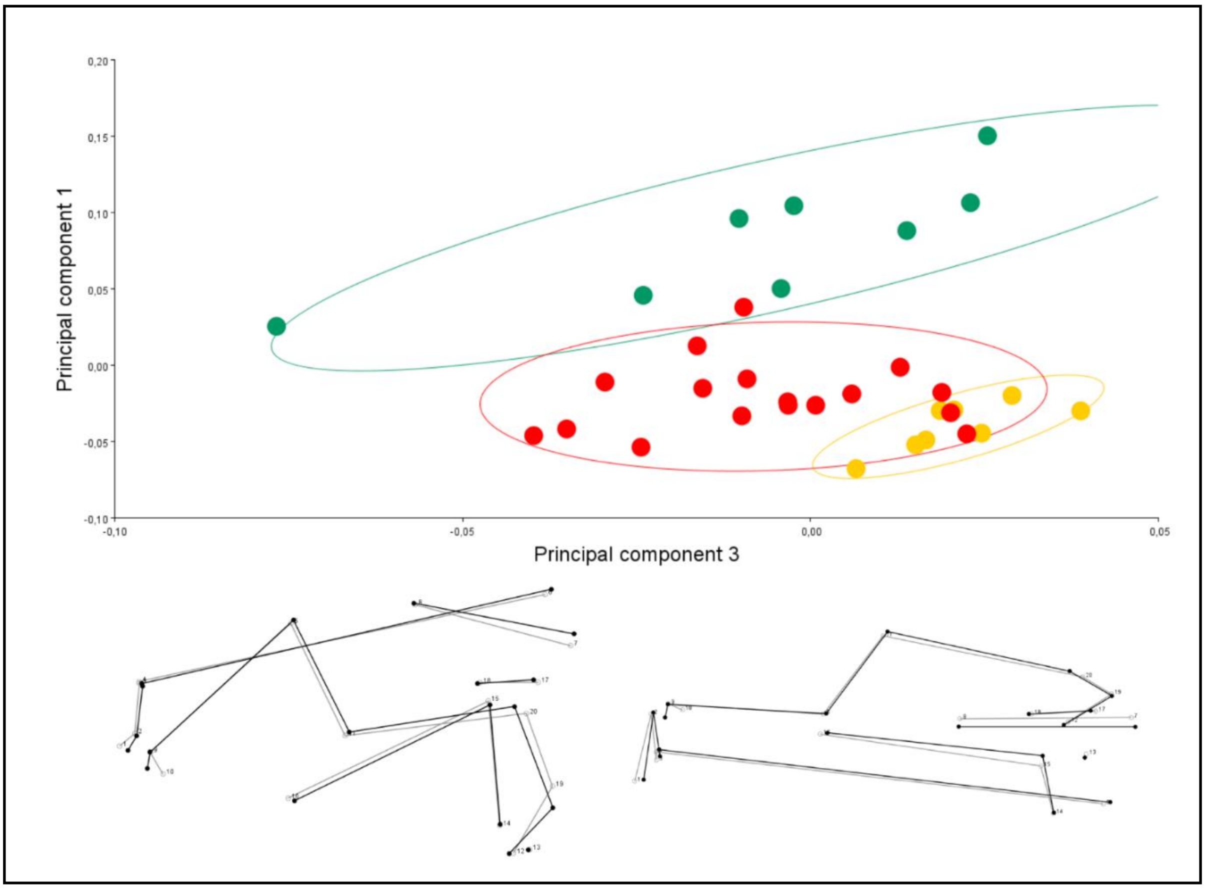

Figure 6. Morphospace formed by PC3 and PC1 considering overall shape in the three species of *Trachycephalus* - *T. nigromaculatus* (red), *T. atlas* (yellow), *T. mambaiensis* (greenish blue). Shapes represent PC3 in 0.05. Black lines represent the target and grey lines the mean shape.

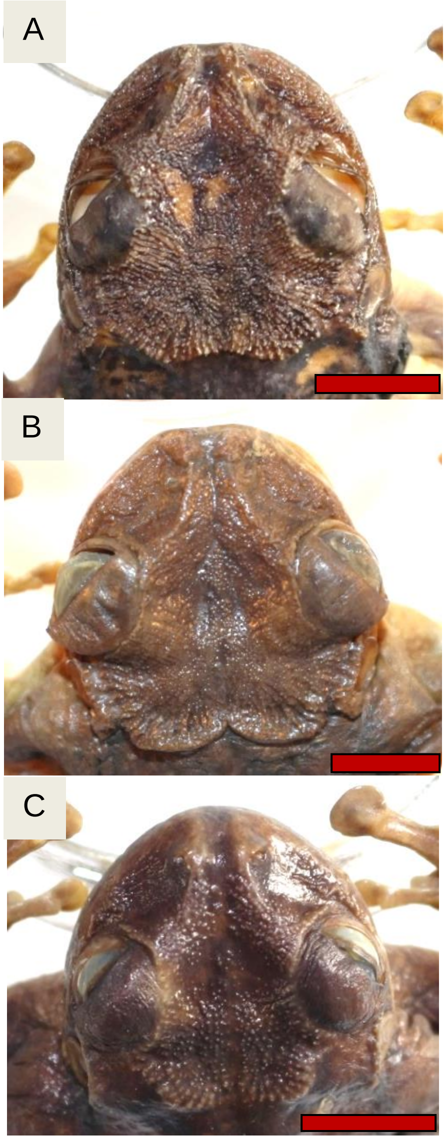

Figure 7. Differences in hyperossification of the skull between (a) A male MNRJ 50991 of *Trachycephalus nigromaculatus*, from Campo dos Goytacazes, Rio de Janeiro, (b) A male MZUSP 74651 of *T. atlas*, from Maracás, Bahia and (c) A male MNRJ 38856 of *T. mambaiensis*, from João Pinheiro, Minas Gerais. Scale: 10mm.

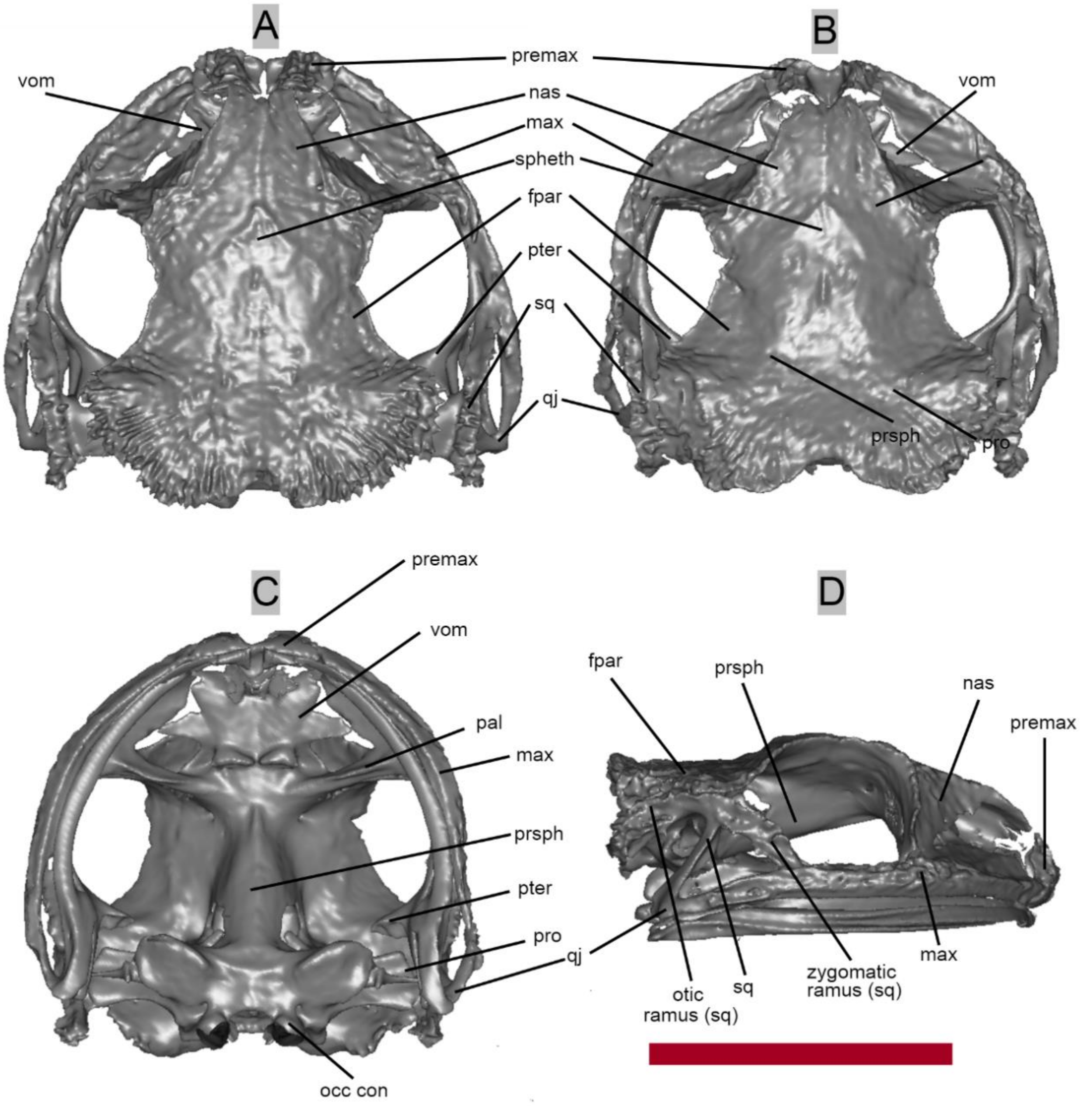

Figure 8. Intraspecific variation of the skull of *Trachycephalus atlas.* (a) Dorsal view of a male CFBH 18811, from Maracás, Bahia (b) Dorsal view of a female MNRJ 19290, from Maracás, Bahia (c) Ventral view of a female MNRJ 19290 (d) Lateral view of a female MNRJ 19290.

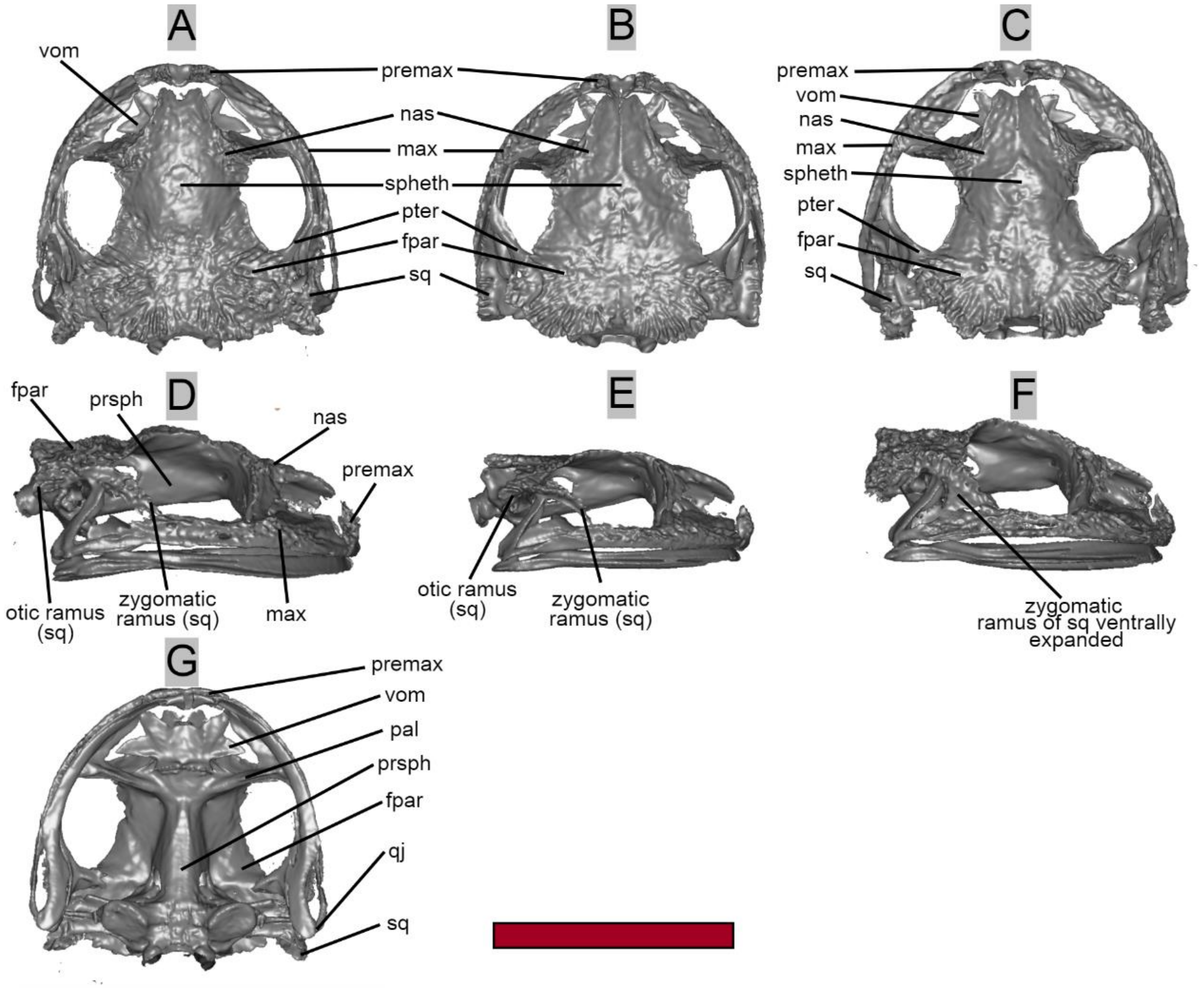

Fig 9. Intraspecific variation of specimens of *Trachycephalus nigromaculatus*. Observe the different of shape of frontoparietals and squamosal between specimens. (a) Dorsal view of skull of a female MNRJ 94296, from Parque Nacional Restinga de Jurubatiba, Macaé, Rio de Janeiro, (b) Dorsal view of skull of a female MNRJ 15661, from Mocambinho, Minas Gerais, (c) Dorsal view of skull of a female CFBH 37285, Petrolândia, Pernambuco, (d) Lateral view of skull of a female MNRJ 94296, from Parque Nacional Restinga de Jutubatiba, Macaé, Rio de Janeiro, (e) Lateral view of skull of a female MNRJ 15661, from Mocambinho, Minas Gerais, (f) Lateral view of skull of a male MNRJ 50990, from Campo de Goytacases, Rio de Janeiro, and (g) Vental view of skull of a female MNRJ 94296, from Parque Nacional Restinga de Jurubatiba, Macaé, Rio de Janeiro. Scale = 20mm. Abbreviations: fpar, frontoparietal; max, maxilla; nas, nasal; pmax, premaxilla; prsph, parasphenoid; pter, pterygoid; qj, quadratojugal; spheth, sphenethmoid; sq, squamosal; vom, vomer.

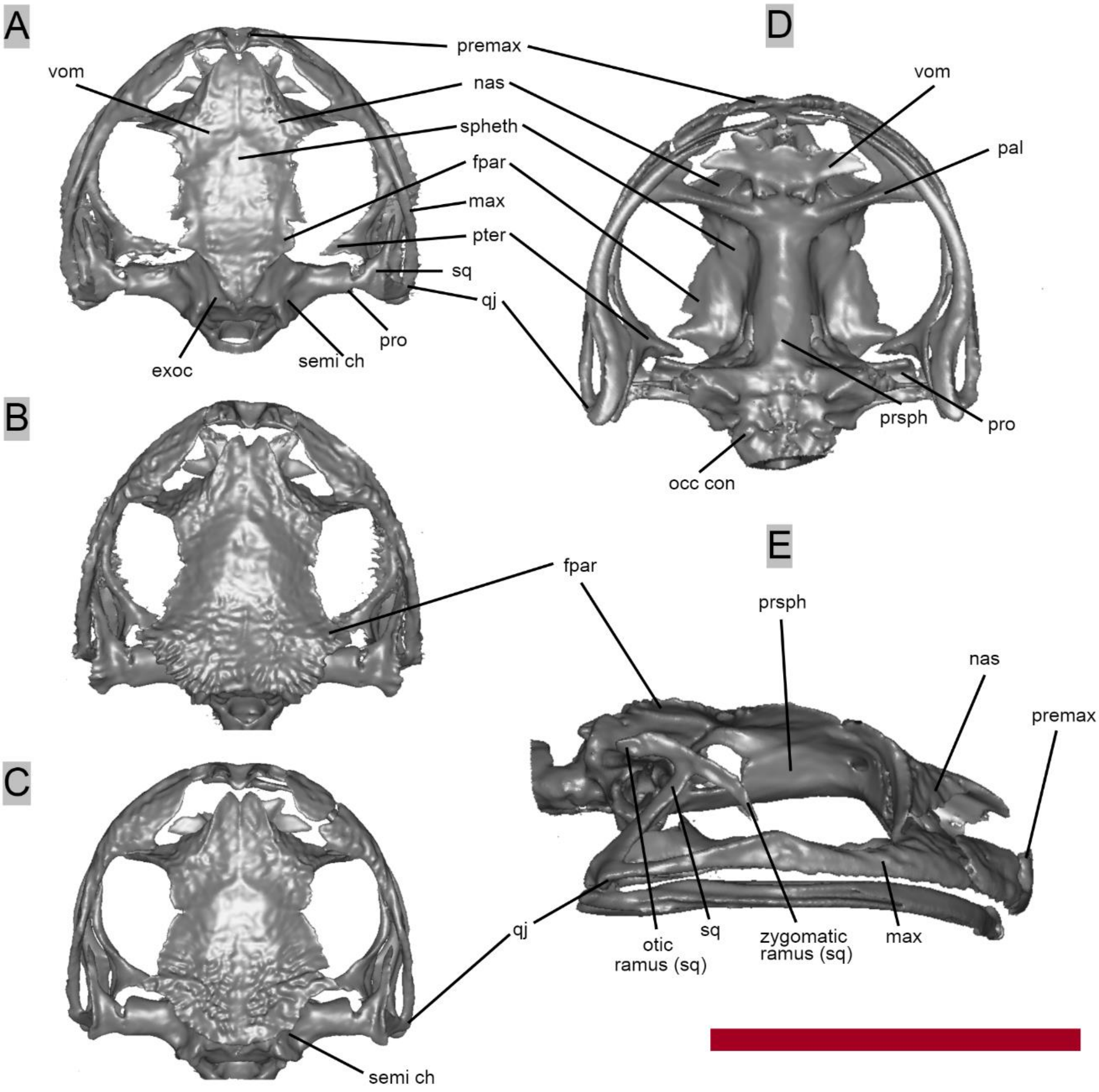

Fig 10. Intraspecific variation of specimens of *Trachycephalus mambaiensis*. Observe the different shapes of frontoparietals in dorsal view between (a) A female RAB3450, from Felixlândia, Minas Gerais, (b) A male MNRJ 38856, from João Pinheiro, Minas Gerais, and (c) A female RAB 3232, from Damianópolis, Goiás. (d) Ventral view of skull of RAB3232. (e) Lateral view of skull of RAB3232. Scale = 20mm. Abbreviations: exoc, exoccipital; fpar, frontoparietal; max, maxilla; nas, nasal; pmax, premaxilla; pro, prootic; prsph, parasphenoid; pter, pterygoid; qj, quadratojugal; spheth, sphenethmoid; sq, squamosal; vom, vomer; pal, palatine; occ cond, occipital condyle.

Appendix 1

Brazilian herpetological collections of specimens used:

Museu Nacional, Rio de Janeiro, Brazil (MNRJ)
Museu de Zoologia da Universidade de São Paulo (MZUSP)
Coleção Herpetológica da Universidade de Brasília (CHUNB)
Coleção Herpetológica do Museu de Zoologia João Moojen (UFV)
Universidade Federal de Sergipe (UFS)
Seção de Herpetologia da Universidade Federal de Minas Gerais (CCT/UFMG)
Coleção Célio Fernando Baptista Haddad (CFBH)
Coleção Herpetológica da Universidade Estadual de Santa Cruz (MZUESC)
Coleção Herpetológica da Universidade Federal da Paraíba (UFPB)

Capítulo 2: **Assessing life-history traits of three poorly studied species of Casque-headed Treefrogs from Brazil through skeletochronology (Hylidae, Lophiohylini).**

Submetido à Journal of Zoology (https://zslpublications.onlinelibrary.wiley.com)

Isabella Parreira[1, 2*], Fernanda Barros Passaglia[1,2], Pedro Paulo de Queiroz[1,3], Anderson Kennedy De-Lima[2,3], Reuber Albuquerque Brandão[1,2,4].

[1] Universidade de Brasília (UnB), Departamento de Engenharia Florestal (EFL), Laboratório de Fauna e Unidades de Conservação (LAFUC), Brasília, DF, Brazil 70910-900

[2] Programa de Pós-graduação em Zoologia, Instituto de Ciências Biológicas, Universidade de Brasília. Campus Darcy Ribeiro - Asa Norte, Brasília, Brazil

[3] Departamento de Ciências Fisiológicas, Instituto de Ciências Biológicas, Universidade de Brasília, Campus Darcy Ribeiro, Asa Norte, Brasília, DF, CEP 70910-900. Brazil.

[4] Museo Argentino de Ciencias Naturales "Bernardino Rivadavia". Sección Herpetologia. Av. Angel Gallardo 470 - C1405DJR - Buenos Aires – Argentina

Abstract

Understanding the interplay between body size, longevity, and sexual maturity is essential for deciphering the reproductive biology and natural history of anurans. Skeletochronology, employing Lines of Arrested Growth (LAG), emerges as a pivotal tool, surpassing conventional methods, as bone cross-sections offer insights into seasonal growth variations driven by a genetically determined circannual rhythm synchronized with the seasonal cycle. In this study, we employed skeletochronology to explore the correlation between body size, longevity, and sexual maturity in *Trachycephalus nigromaculatus, T. atlas,* and *T. mambaiensis*. Age estimation through LAG counting revealed disparities in estimated age and sexual maturity among these species. *T. nigromaculatus* exhibited an average estimated age of 3.1 ± 1.5 LAGs, *T. atlas* showed 2.9 ± 1.6 LAGs, and *T. mambaiensis* displayed 2.4 ± 0.9 LAGs on average. Males of *T. nigromaculatus* and *T. atlas* reached sexual maturity at two LAGs, while *T. mambaiensis* males at one LAG. Females of all three species demonstrated developed ovaries by three LAGs. Significant correlations between snout-vent length (SVL) and age were observed for *T. nigromaculatus* and T. atlas, but not for *T. mambaiensis. T. atlas* exhibited slower growth compared to *T. nigromaculatus*. *T. nigromaculatus* specimens were collected year-round (except for April, July, and August); *T. atlas* and *T. mambaiensis* were predominantly found during the rainy season. These findings suggest distinct growth patterns and seasonal behavior among *Trachycephalus* species studied. Skeletochronology using LAGs facilitates investigations into the evolutionary-ecological processes and natural history of *Trachycephalus* and other explosive breeder species, utilizing preserved museum specimens.

Keywords: body-size, *Trachycephalus atlas, Trachycephalus mambaiensis, Trachycephalus nigromaculatus,* tropical regions, Von Bertalanffy growth model.

Introduction

The complex correlation between body size, growth patterns, longevity, and age in anurans underscores the complexity of their life history strategies and ecological adaptations (Morrison & Hero 2003, Liao et al. 2016), which are controlled by several evolutionary, genetic, ecological, and environmental factors (Castanet 1993, Feilich, 2016). These traits play pivotal roles in anuran biology, influencing diverse life-history characteristics such as physiological adjustments, territoriality, predator-prey interactions, reproductive strategies, distribution, habitat preferences, sexual maturity, and growth rate dynamics (Arantes et al., 2015; Rebouças et al., 2019; Baraquet et al., 2021; Barbault, Castanet, & Pilorge, 1980; Liao & Lu, 2011; Erismis, 2018).

The indeterminate growth observed in anurans often correlates their body size with age (Li et al., 2010; Arantes et al., 2015; Otero et al., 2017a, 2017b), highlighting the significance of understanding this relationship for elucidating anuran evolutionary-ecological processes (Shine, 1988; Moen & Wiens, 2009). This association offers researchers deeper insights into the mechanisms governing population dynamics, species interactions, and ecosystem functioning within anuran habitats (Guo et al., 2019; Amado et al., 2020). Moreover, the observed correlation between body size and age in anurans reflects fundamental aspects of their reproductive biology and natural history, as investigated within the group (Miaud, Guyétant & Elmberg, 1999).

Skeletochronology, employing Lines of Arrested Growth (LAG), has emerged as a prevalent and effective method for unraveling growth and age dynamics in anurans, surpassing conventional techniques like capture-mark-recapture (Sinsch, 2015). LAGs typically result from variations in individual growth rates induced by seasonal fluctuations, serving as temporal markers of growth dynamics (Castanet et al., 1993), visualized in bone cross-sections (Castanet, 1982; Castanet and Smirina, 1990). LAG formation ultimately stems from a genetically based, circannual rhythm, synchronized with, and reinforced by the seasonal cycle under natural conditions (Castanet, 1993). The scarcity of skeletochronological investigations is noted in amphibians inhabiting tropical regions, where growth may still be influenced by periodicity due to rainy and dry seasons (Kumbar & Pancharatna, 2002).

The utilization of the Skeletochronology method arises from challenges inherent encountered in traditional studies, particularly with species characterized by low population densities or those that are difficult to sample (Halliday & Verrell, 1988). In the early investigations of growth marks, round bones such as the femur or humerus emerged as the preferred choice (Kleinenberg & Smirina, 1969; Smirina, 1972a, b; Castanet & Smirina, 1990; Castanet et al., 1993); however, this method demanded the sacrifice of an unacceptably large number of individuals or resulted in damage to museum specimens (Smirina, 1972a; Castanet, 2002). Since Smirina (1972a), the use of phalanges for age determination has provided a less invasive alternative, yielding comparable information to long bones (Smirina, 1972a; Gibbons & McCarthy, 1983; Rozenblut & Ogielska, 2005), while minimizing harm to museum specimens and reducing the need to sacrifice living specimens.

The clade consisting of *Trachycephalus nigromaculatus* Tschudi, 1838, *T. atlas* Bokermann, 1966, and T*. mambaiensis* Cintra, Silva, Silva, Garcia, & Zaher, 2009, comprises poorly studied large-sized tree frogs. These species mainly inhabit dry forest habitats (Roberto et al., 2011; Neta, Silva & Ávila, 2018; Silva et al., 2020) and exhibit extensive processes of co-ossification in the cranium (Bokermann, 1966; Trueb, 1970a; Cintra et al., 2009; Blotto et al., 2021). Records indicate their presence in restinga phytophysiognomy within the Atlantic Rain Forest (Lutz, 1954; Freitas & Lima, 2009; Dias et al., 2010; Almeida, Gasparini & Peloso, 2011), forested Caatinga (Borges-Nojosa & Arzabe, 2005; Roberto et al., 2011; Neta et al., 2018), and dry forests in the Cerrado (Dayrell et al., 2012; Vaz-Silva et al., 2020) biomes. The occurrence of these species in seasonal environments likely influences their annual growth patterns (Marangoni et al., 2009).

To date, the investigation of growth curves among *Trachycephalus* species remains limited, representing a significant gap in our understanding of the life history within this genus. This study aims to examine the correlation between body size, longevity, and sexual maturity in individuals of *Trachycephalus nigromaculatus, T. atlas,* and *T. mambaiensis* by employing the Skeletochronology method using Lines of Arrested Growth (LAGs).

Material and methods

Data collection

All specimens analyzed herein were collected during previous fieldwork and deposited in several Brazilian herpetological collections (see Supporting Information for individual numbering and museum acronyms). Since these species are uncommon in collections, we examined 33 specimens of *Trachycephalus nigromaculatus* (14 females, 14 males, five juveniles), 14 of *T. atlas* (four females, five males, and four juveniles), and 12 of *T. mambaiensis* (three females, eight males, and one juvenile), from 34 localities (Fig. 1), deposited in the Coleção de Anfíbios do Museu Nacional, Universidade Federal doRio de Janeiro (MNRJ), Universidade Federal de Sergipe (UFS), Universidade Federal de Minas Gerais (UFMG), Coleção Herpetológica da Universidade de Brasília (CHUNB), Coleção Herpetológica da Universidade Estadual de Santa Cruz (MZUESC), Coleção Herpetológica do Museu de Zoologia João Moojen (UFV), Coleção do Laboratório de Fauna e Unidades de Conservação (LAFUC-UnB), Coleção de Anfíbios Célio F. B. Haddad (CFBH), and Coleção Herpetológica da Universidade Federal do Rio Grande do Norte (UFRN). All individuals were sexed by direct examination of primary (gonads, eggs) or secondary sexual characters (presence of vocal sac and nuptial pad in males). We measured snout-vent length (SVL) for all specimens and considered the smaller size for males as the smallest individual having developed vocal sacs and for females the smallest individual having developed gonads (Tessa et al., 2019).

Skeletochronology

The McCreary, Pearl & Adams (2008) protocol (with modifications) was employed to estimate the age of specimens. The third phalanx of finger IV was excised, fixed in 70% ethanol for a minimum of 24 hours, and decalcified in 5% EDTA for 14 days (modified), with solution replacement on the seventh day. Subsequently, the tissue was dehydrated and cleared in sequential solutions: 90% ethanol, 100% ethanol, 100% ethanol with xylene substitute, and xylene substitute. Following clearing, the specimens were embedded in paraffin for infiltration. Paraffin blocks were sectioned into 5µm slices using a Leica® rotary microtome. The sections were mounted on glass slides and oven-dried at 60°C for four to six hours.

A total of 1180 glass slides from the three species were examined, and those offering optimal visualization under an optical microscope were selected for the observation and counting of Lines of Arrested Growth (LAG) and metamorphosis lines (LM), following the approach proposed by Sinsch, Oromi & Sanuy (2007). Metamorphosis lines were disregarded, and specimens displaying only these lines were classified as age class 0+. Double lines were treated as a single LAG, with each LAG corresponding to one year, as proposed by Sinsch (2015). The counting procedures were independently performed by two observers (IP and FBP) to minimize idiosyncratic biases in the final count.

Estimated age analyses

We used the Pearson product-moment correlation coefficient to verify the relationship between age and snout-vent length (SVL) and differences between age, snout-vent length (SVL), and sexes. Descriptive analyses were performed between age and the presence of egg mass (in females) or a nuptial pad (in males) to indicate age at sexual maturity. Furthermore, we evaluated the adjustment of the average growth of species with the nonlinear Von Bertalanffy (1938) growth model, except for *Trachycephalus mambaiensis* due to the small sample size. We performed all statistical analyses using the R software (R Studio v. 4.3.1., 2023) with a significance level of 5%.

Annual records

The annual records of *Trachycephalus nigromaculatus*, *T. atlas*, and *T. mambaiensis* were inferred from the frequency of collection records that were grouped by month for males, females, and juveniles. Circular statistics were employed to describe the annual records between the species (Jammalamadaka & Sengupta; 2001; Pewsey, Neuhäuser & Ruxton, 2013). We removed from the analysis individuals who were not collected during activity (e.g. animals found during faunal rescue projects under river damming). The duration of dry and rainy seasons of each locality was retrieved from Alvares et al., (2013).

Results

Estimated ages

All specimens within the studied clade exhibited identifiable bone structures enabling precise age determination through the counting of Lines of Arrested Growth (LAGs). *Trachycephalus nigromaculatus* had an average estimated age of 3.1 ± 1.5 LAGs (0–6, modal = 3), *T. atlas* had an average estimated age of 2.9 ± 1.6 LAGs (0–6, modal = 3) and *T. mambaiensis* presented an average estimated age of 2.4 ± 0.9 LAGs (1–4, modal = 2 and 3) (Table 1). Males of *Trachycephalus nigromaculatus* exhibited 1–6 LAGs, whereas females presented 2–6 LAGs; males reached sexual maturity at two-year-old, while females were mature at the age of three (Table 1). For *Trachycephalus atlas,* we recorded males with 2–4 LAGs, whereas we recorded females with 3–6 LAGs, but none with four LAGs; males were maturity at two-yearsold, while females presented developed ovaries at the age of three (Table 1). Males of *Trachycephalus mambaiensis* presented 1–3 LAGs, whereas we recorded with 2–4; males were mature at one-year-old, while females reached sexual maturity at the age of three (Table 1).

There is positive correlation between snout-vent length (SVL) and the estimated age of specimens for *Trachycephalus nigromaculatus* (t = 2.65, p < 0.01, Fig. 2A) and *T. atlas* (t = 3.09, p < 0.009, Fig. 2B), but not for *T. mambaiensis* (t = 0.86, p= 0.41; Fig. 2C). Females of *Trachycephalus nigromaculatus* and *T. atlas* showed positive correlation between body-length and age (t = 2.10, p < 0.01, Fig. 2). We do not find differences in body-length between females and males of *Trachycephalus nigromaculatus* (p = 0.4, f = 0.5), *T. mambaiensis* (p = 0.9, f < 0.01), and *T. atlas* (p = 0.6, f = 0.3).

Juveniles of *Trachycephalus nigromaculatus* presented a mean body length of 61.5 ± 11.2mm (range 37.6–65.5). Females showed higher mean body length than males in all LAGs recorded. With two LAGs, females presented mean body-length of 96.5 mm (n = 1), and males of 83.9 ± 1.7 mm (81.4–85.5), with three LAGs females presented mean body-length of 85.2 ± 6.7 mm (70.4–104.9) and males of 83.9 ± 1.8 mm (81.4–85.5), with four LAGs females presented mean body-length of 89.8 ± 3.3 mm (85.9–94.0) and males of 81.3 ± 3.3 mm (76.4–86.1) and with five LAGs females presented mean body-length of 82.5 ± 9.6 mm (72.9–92.1) and males of 77.6 ± 3.1 mm (73.3–80.1); oldest males presented mean body-length of 88.6 ± 1.6 mm (87.0–90.3)

The mean of juveniles' body length of *Trachycephalus atlas* was 62.8 mm ± 3.5 (59.0–61.2). Males with two LAGs showed the largest body length of 86.5 ± 2.6 mm (84.6–88.4), bigger than all females recorded. Females with three LAGs were the largest, with a mean body of 80.5 ± 0.05 mm (80.4–80.5), whereas males at the same age presented a mean body length of 77.9 mm (n = 1). The oldest female presented an SVL of 85.5 mm.

The mean body length of *Trachycephalus mambaiensis* with one LAG was 68.3 ± 15.6 mm (57.2–79.3 mm). Males with two LAGs showed a mean body length of 69.9 ± 6.3 mm (64.3–76.8) being larger than a female of the same age, with 63.2 mm (n = 1). Females with three LAGs were the largest, with a mean body length of 77.8 mm (n = 1), whereas males at the same age had a mean of 74.3 ± 10.9 mm (67.9–86.9). The oldest female presented a SVL of 77.5 mm.

The relationship between the age and body length of the species correctly fitted the Von Bertalanffy (1938) growth model (Fig. 3). Based on the growth coefficient value (K), the growth rate of *Trachycephalus nigromaculatus* was faster (K= 1.24; 98% confidence interval) than *T. atlas* (K=0.31; 95% confidence interval). The growth model indicates that *Trachycephalus nigromaculatus* showed accelerated growth before maturity, presenting lower growth rates after two LAGs for females and one LAG for males (Fig. 3A). *T. atlas* presented a constant growth rate, without a tendency to stabilize (Fig. 3B).

Annual Records

Trachycephalus nigromaculatus specimens were collected year-round, with no records in April, July, and August (dry season). Males were more frequently collected during the rainy season, with a few records even in May, June, and July. Female records were primarily during the rainy season (October), except for one record in September (at the end of the dry season). Juveniles were exclusively found during the rainy season (January, February, and October), except for one record in May. Females with egg masses were recorded in March (n = 1), October (n = 1), and November (n = 3), while males with developed nuptial pads were recorded in September (n = 1), December (n = 3), and January (n = 1).

All records of *Trachycephalus atlas* were during the rainy season, from mid-December to mid-April. Males were collected from December to February, females were found in January and April, and juveniles were found in February and March. Males with developed nuptial pads were recorded in December (n = 2).

Records of *Trachycephalus mambaiensis* ranged from mid-dry season (July, n = 1) to early January, during the rainy season. All male and female records occurred during the rainy season, more frequently in December for males and October for females. The juvenile record was in the dry season (July). Females with egg masses were recorded in October (n = 2), while males with developed nuptial pads were recorded in December (n = 2) and January (n = 2).

Discussion

Although age estimations should be ideally addressed on closed populations (Arantes et al. 2015, Rebouças et al. 2019), we used individuals belonging to similar morphoclimatic regions, likely reducing eventual variations in growth and survival patterns between populations. Since these species are poorly represented in collections, the use of combined individuals proved to be effective in describing general patterns for access differences on species survival and growth patterns. The recovered patterns are useful for describe differences on cranial ornamentation between species based on their age and to report the presence of LAGs in this poorly studied clade.

Our study highlights the usefulness of LAGs as a valuable tool for estimating the life-history traits of these three large-sized casque-headed frogs in seasonal habitats in South America. Specifically, the association between age and external morphology provides insights into longevity, age at sexual maturity, variation in body length, growth rate, and reproductive activity within these species, that should be explored in further studies.

The longevity and age at sexual maturity estimated for *Trachycephalus nigromaculatus, T. atlas,* and *T. mambaiensis* are similar to previous studies reported for other tropical frogs (Li et al., 2010; Lindquist, Redmer & Brantner, 2012; Arantes et al., 2015). We lacked access to males of *Trachycephalus atlas* at the age of one LAG. Nevertheless, *Trachycephalus mambaiensis* emerges as the smallest species examined in this study, displaying small longevity and the early development of nuptial pads in males (with one LAG). Generally, smaller-sized species tend to exhibit shorter lifespans and attain sexual maturity earlier compared to larger species (Tessa et al., 2017) and the development of nuptial pads is driven by androgens levels (Epstein & Blackburn, 1997; Brizzi et al., 2003), with these secondary sexual characteristics associated with sexual maturation (Zhang et al., 2013) and male mating success (Orton et al., 2022).

We found a correlation between body length and the estimated age of specimens for *Trachycephalus nigromaculatus* and *T. atlas.* Females of *Trachycephalus nigromaculatus* have a larger SVL compared to males, with the same number of LAGs; in *T. atlas* and *T. mambaiensis,* males during early stages of development (1–2 LAGs) presented larger body lengths than females, with the same number of LAGs. Males of these species tend to attain sexual maturity at younger ages compared to females, which may be influenced by distinct ecological conditions (Morrison & Hero, 2003) and sexual selection (Gibbons & McCarthy, 1983). While both sexes strive to maximize their reproductive fitness, males have the potential to enhance their reproductive success by attaining sexual maturity earlier and mating with multiple females (Sá et al., 2020; Dittrich & Rodel, 2023).

Conversely, females should trade off their sexual maturity age in favor of a larger body size, aiming to achieve larger reproductive output (Gibbons & McCarthy, 1983).

On the other hand, we did not find sexual dimorphism among the three species analyzed here. In many anuran species, sexual dimorphism in body size is a prevalent phenomenon, with females typically exhibiting larger sizes than males (Shine, 1989). This dimorphism is commonly attributed to the heightened reproductive investment of females, characterized by increased egg production. Consequently, larger female body sizes are favored to accommodate larger clutch sizes (Gibbons & McCarthy, 1983). However, the process of mate selection in anurans is substantially influenced by male-male competition for access to females, mainly explosive breeding species (Emlen & Oring, 1977). This competitive dynamic often results in the preferential selection of larger males, who possess competitive advantages in securing mating opportunities (Kupfer, 2007). Consequently, both sexes are subject to selective pressures favoring larger body sizes, though the intensity of these pressures may vary between sexes and species, a trend that may have been affected by our small sample size.

We found a higher growth rate in *Trachycephalus nigromaculatus* and the growth curve of *T. atlas* did not allow us to estimate stabilization in any age. Tendency to growth stabilization is commonly recorded in other tropical species (Marangoni et al., 2009; Stănescu et al., 2016). Different from *Thoropa miliaris, a* species endemic to the Atlantic Rain Forest (Rebouças et al. 2017), *Trachycephalus nigromaculatus* showed growth stabilization and a growth model type I (Sebens, 1987), where growth present an asymptotic pattern influenced by food availability and physiological factors, with the maximum size fluctuating based on these conditions (Sebens, 1987). Regarding species inhabiting dry forests the occurrence of growth stabilization has been documented for some species (Stănescu et al., 2016; Pascual-Pons et al., 2017), but not for other ones (Khonsue, Matsui & Misawa, 2000; Marangoni, Tejedo & Cogălniceanu, 2021). Additionally*, Trachycephalus atlas* presented an undetermined growth model type III (Sebens, 1987), where growth does not exhibit a fixed size limit but tends to decelerate over time. Organisms presenting a type III growth curve tend to retain plasticity, enabling significant alterations in growth rate throughout life in response to habitat conditions, a strategy that allows successful thriving in challenging environments, such as the semi-arid Brazilian Caatinga.

Although we have not access to the activity period of each collected specimen, we suggest that females recorded with egg mass and males recorded with developed nuptial pads were in reproductive activity when collected. We observed that the activity peak of species with explosive breeding behavior, such as *Trachycephalus*, is related to the occurrence of heavy rainfall, often at the beginning of the rainy season (Aichinger, 1987; Haddad & Prado, 2005). Air temperature, relative air humidity, and total monthly rainfall are positively correlated with the reproductive activity of neotropical frogs, a pattern more markedly in seasonal biomes (Duellman & Trueb, 1994; de Sá, Zina & Haddad, 2014).

Finally, investigating the correlation between body size, longevity, and sexual maturity may be important for assessing life-history traits in casque-headed species, particularly those that restrict their activity to the rainy season. The use of skeletochronology using LAGs counting through preserved specimens allowed us to access some critical natural history aspects of the uncommon and poorly studied species in the *Trachycephalus nigromaculatus* species clade. Our study highlights the relevance of specimens housed in museums for ecological and evolutive studies, including taxonomic groups that are hard to find in nature

Acknowledgements

We thank to ICMBio (86764/1), ICMBio (Mambaí, Goiás), Sítio Boca do Mato, Mambaí, Goiás (Lauana, Raoni), Cachoeira Paraíso do Cerrado, Damianópolis, Goiás (Silvano) for support in fieldworks and to José Pombal Jr (MNRJ), Renato Faria (UFS), Thiago Ribeiro Carvalho (UFMG), Guarino R. Colli (CHUNB), Victor Dill Orrico (MZUESC), Renato Feio (UFV), Célio F. B. Haddad (CFBH), and Elisa Freire (UFRN) for permissions of use of specimens; to the Coordenação de Aperfeiçoamento de Pessoal de Nível Superior (CAPES, DS-Programa de Demanda Social/ process #88887.918726/2023-00) which promoted grant to IP, to the Conselho Nacional de Desenvolvimento Científico e Tecnológico (CNPq) which promoted productivity grant to RAB (process #306644/2020-7) and pos-doc grant to RAB (Edital DPG/UnB Nº 0009/2023) from Universidade de Brasília (UnB) This sudy was financially supported by Fundação de Apoio à Pesquisa do Distrito Federal (FAPDF/ Edital 005/2022) and and Programa de Pós-graduação em Zoologia (PGZoo/UnB).

Author Contributions Statement

IP performed research and wrote the paper. IP and FBP analyzed data. IP, FBP, PPQ and AKde-L contributed with methods. All authors reviewed the manuscript.

References

Alvares, C. A., Stape, J. L., Sentelhas, P. C., Gonçalves, J. D. M., & Sparovek, G. (2013). Köppen's climate classification map for Brazil. Meteorologische Zeitschrift, 22(6), 711-728.

Aichinger, M. (1987). Annual activity patterns of anurans in a seasonal neotropical environment. *Oecologia* **71**, 583–592. https://doi.org/10.1007/BF00379302

Almeida, A. de P., Gasparini, J. L., Peloso, P. L. V. (2011). Frogs of the state of Espírito Santo, southeastern Brazil - The need for looking at the 'coldspots'. *Check List,* **7**(4): 542– 560.

Amado, T., Martinez, P. A., Pincheira-Donoso, D., & Olalla-Tárraga, M. (2020). Body size distributions of anurans are explained by diversification rates and the environment. Global Ecology and Biogeography. 00. 1-11. 10.1111/geb.13206.

Arantes, I. C., Vasconcellos, M. M., Boas, T. C. V., Veludo, L. B. A. & Colli, G. R. (2015). Sexual dimorphism, growth, and longevity of two toad species (Anura, Bufonidae) in a Neotropical Savanna. *Copeia* **103** (2), 329–342.

Bancroft, J. D. & Gamble, M. (2002). Theory and practice of histological techniques. 5th. Ed. Edinburgh. Churchill Livingstone Pub. 593–620.

Baraquet, M., Pollo, F. E., Otero, M. A., Grenat, P. R., Salas, N. E & Martino, A. L. (2021). Body size, age and growth in males' populations of *Boana pulchella* (Anura, Hylidae). *Anais da Academia Brasileira de Ciências,* **93** (4).

Barbault, R., Castanet, J. & Pilorge, T. (1980). On the use of skeletochronology in demographic studies of amphibian and lizard populations. *Bulletin de la Societe Zoologique de France-Evolution et Zoologie* (105) 347–354.

Bokermann, W. C. A. (1966). Una nueva especie de *Trachycephalus* de Bahia, Brasil (Amphibia, Hylidae). *Neotropica.* La Plata **12**: 120–124.

Borges-Nojosa, D. M., Arzabe, C. (2005). Diversidade de anfíbios e répteis em áreas prioritárias para a conservação da caatinga. *In Análise das variações da biodiversidade do bioma caatinga: suporte a estratégias regionais de conservação* (Araújo, F. S., Rodal, M. J. N. & Barbosa, M. R. V. eds.). Ministério do Meio Ambiente, Secretaria de Biodiversidade e Florestas, Brasília, 227–241.

Blotto, B. L., Lyra, M. L., Cardoso, M. C., Trefaut Rodrigues, M., Dias, R. I., Marciano-Jr, E., Dal Vechio, F., Orrico, V. G., Brandão, R. A., Lopes de Assis, C., Lantyer-Silva, A. S., Rutherford, M. G., Gagliardi-Urrutia, G., Solé, M., Baldo, D., Nunes, I., Cajade, R., Torres, A., Grant, T., Jungfer, K.-H., da Silva, H. R., Haddad, C. F., Faivovich, J. (2021). The phylogeny of the Casque-headed Treefrogs (Hylidae: Hylinae: Lophyohylini). *Cladistics,* **37**: 36–72.

Brizzi, R., Delfino, G., & Jantra, S. (2003). An overview of the breeding glands. In B. G. M. Jamieson (Ed.), Reproductive biology and phylogeny. *Science Publishers Inc,* 253–317.

Castanet, J., H. Francillon-Vieillot, F. J. Meunier, and A. de Ricqlès. 1993. Bone and individual aging **7***:* 245–283 in B. K. Hall (ed.), *Bone: Bone Growth.* Boca Raton. CRC Press.

Castanet, J. (2002). Amphibiens et reptiles non aviens: um materiel de choix en squelettochronogie. *Bulletin De La Societe Zoologique De France-Evolution Et Zoologie*, **103**, 21–40.

Cintra, C. E. D., Silva, H. L. R, Silva, N. J., Garcia, Jr. P. C. de A., Zaher, H. (2009). A new species of *Trachycephalus* (Amphibia, Anura, Hylidae) from the state of Goiás, Brazil. *Zootaxa* **1975**: 58–68.

Dayrell, J. S., Fernandes, V. D., Moura, M. R., Feio, R. N. (2012). New records of *Trachycephalus mambaiensis* (Amphibia: Hylidae) from a cerrado region in Minas Gerais state, Brazil. *Check List*, **8**(2): 269–271.

de Sá, F. P., Zina, J., & Haddad, C. F. B. (2014). Reproductive Dynamics of the Neotropical Treefrog *Hypsiboas albopunctatus* (Anura, Hylidae). Journal of Herpetology, **48** (2), 181–185. https://doi.org/10.1670/12-193.

Dias, I. R., Vilaça, T. R. A., Silva, J. R. S., Barbosa, R. S., Solé, M. (2010). Amphibia, Anura, Hylidae, *Trachycephalus nigromaculatus* Tschudi, 1838: Distribution extension. *Check List*, **6**(3): 212–213.

Dittrich, C., & Rödel, M-O. (2023). Drop dead! Female mate avoidance in an explosively breeding frog, *Royal Society Open Science*, **10** (230742). https://doi.org/10.1098/rsos.230742

Emlen, S. T, & Oring, L. W. (1977). Ecology, sexual selection, and the evolution of mating systems. *Science* **197**, 215–223. doi:10.1126/science.327542.

Epstein, M. S., & Blackburn, D. G. (1997). Histology and histochemistry of androgen-stimulated nuptial pads in the leopard frog, Rana pipiens, with notes on nuptial gland evolution. Canadian Journal of Zoology, **75**(3), 472–477.

Erismis, U. (2018). Age, Size, and Growth of the Turkish Endemic Frog *Pelophylax caralitanus* (Anura: Ranidae). *The Anatomical Record.* **301**. 10.1002/ar.23758.

Feilich, K. L. (2016). Correlated evolution of body and fin morphology in the cichlid fishes. Evolution, **70**: 2247–2267. https://doi.org/10.1111/evo.13021.

Freitas, M.A., Lima, T. O. (2009). *Trachycephalus nigromaculatus* (Blackspotted Casque-headed Tree Frog). *Herpetological Review*, **40**(3): 363.

Frost, D. R. Amphibian Species of the World: An Online Reference. Version 5.5 (March, 2024). Electronic Database on https://amphibiansoftheworld.amnh.org/.

Gibbons, M. M. & McCarthy, T. K. (1983). Age determination of frogs and toads (Amphibia, Anura) from Northwestern Europe. *Zoologica Scripta*, **12**, (2), 145–151.

Guo, C., Gao, S., Krzton, A., & Zhang, L. (2019). Geographic body size variation of a tropical anuran: effects of water deficit and precipitation seasonality on Asian common toad from southern Asia. *BMC Evolutionary Biology*, **19** (208). https://doi.org/10.1186/s12862-019-1531-z

Haddad, C. F. B. & Prado, C. P. A. (2005). Reproductive modes in frogs and their unexpected diversity in the Atlantic Forest of Brazil. *BioScience* **55**: 207–217.

Halliday, T.R. & Verrell, P. A. (1988). Body Size and Age in Amphibians and Reptiles. *Journal of Herpetology,* **22** (3), 253–265.

Jammalamadaka, S. R., & Sengupta, A. (2001). Topics in circular statistics. *Open Journal of Statistics*, **5** (4).

Khonsue, W., Matsui, M., & Misawa, Y. (2009). Age Determination by Skeletochronology of *Rana nigrovittata,* a Frog from Tropical Forest of Thailand. *Zoological Science.* **17.** 253–257. 10.2108/zsj.17.253.

Kumbar, S. M., & Pancharatna, K. (2002). Annual growth layers in the phalanges of the Indian Skipper Frog *Rana cyanophlyctis* (Schn.). *Copeia:* 870–872

Kupfer, A. (2007). Sexual size dimorphism in amphibians: an overview. In Fairbairn, D.J, Blanckenhorn, W. & Szekely T. Sex, size and gender roles: evolutionary studies of sexual size dimorphism. *Oxford University Press*, 50–59.

Li, C., Liao, W. B., Yang, Z. S., & Zhou, C. Q. (2010). A skeletochronological estimation of age structure in a population of the Guenther's frog, *Hylarana guentheri*, from western China. *Acta Herpetologica,* **5**, 1–11.

Liao, W. B. & Lu, X. (2011). Age structure and body size of the Chuanxi Tree Frog *Hyla annectans chuanxiensis* from two different elevations in Sichuan (China). *Zoologischer Anzeiger,* **248**, 255– 263.

Lindquist, E., Redmer, M., & Brantner, E. (2012). Annular bone growth in phalanges of five Neotropical Harlequin Frogs (Anura: Bufonidae: *Atelopus*). *Phyllomedusa: Journal of Herpetology*, 11(2), 117–124. DOI: 10.11606/issn.2316-

Lutz, B. (1954). Anfíbios anuros do Distrito Federal. *Memórias do Instituto Oswaldo Cruz*, **52**(1): 155–216.

Marangoni, F., Schaefer, E., Cajade, R. & Tejedo, M. (2009). Growth-Mark Formation and Chronology of Two Neotropical Anuran Species. *Journal of Herpetology.* **43**. D: 546–550. 10.1670/08-230R1.1.

Marangoni, F., Tejedo, M. & Cogălniceanu, D. (2021). Can age and growth patterns explain the geographical variation in the body size of two toad species? *An. Acad. Bras. Cienc.* **93**(2): e20190470 DOI 10.1590/0001-3765202120190470

McCreary, B., Pearl, C. A. & Adams, M. J. (2008). A protocol for aging anurans using skeletochronology. *Geological Survey Open-File Report1,* **1209**, 1–38.

Miaud, C., Guyétant, R & Elmberg, J. (2006). Variations in life-history traits in the common frog *Rana temporaria* (Amphibia: Anura): A literature review and new data from the French Alps. Journal of Zoology. **249**. 61–73.

Moen, D. S., & Wiens, J. J. (2009). Phylogenetic evidence for competitively driven divergence: body-size evolution in Caribbean treefrogs (Hylidae: *Osteopilus*). Evolution **63**: 195–214.

Morrison, C., & Hero, J. M. (2003). Geographic variation in life-history characteristics of amphibians: a review. *Journal of Animal Ecology*, **72** (2), 270–279. doi:10.1046/j.1365-2656.2003.00696.x

Neta, A. F. S., Silva, M. C., Ávila, R. W. (2018). Herpetofauna da Bacia Hidrográfica do Rio Salgado, Estado do Ceará, Nordeste do Brasil. *Boletim do Museu de Biologia Mello Leitão*, **40**(1): 23–48.

Orton, F., Roberts-Rhodes, B., Moore, E., Whatley, C., & Tyler, C. R. (2023). Nuptial pad (“breeding gland”) morphology is related to non-random mating in wild male common frogs (*Rana temporaria*). *Ethology*, **129**: 232–239. https://doi.org/10.1111/eth.13361

Otero, M. A., Baraquet, M., Pollo, F., Grenat, P., Salas, N. & Martino, A. (2017a). Sexual size dimorphism in relation to age and growth in *Hypsiboas cordobae* (Anura: Hylidae) from Córdoba, Argentina. *Herpetological Conservation and Biology,* **12**, 141–148.

Otero, M. A., Valetti, J. A., Bionda, C. L., Salas, N. E. & Martino, A. L. (2017b). Are ploidy and age size-related? A comparative study on tetraploid *Pleurodema kriegi* and octoploid *P. cordobae* (Anura: Leptodactylidae) from Central Argentina. *Zoologischer Anzeiger,* **268**, 136–142.

Pascual, M., Oromí, N., Pujol-Buxó, E., Fibla, M., Sanuy, D. & Montori, A. (2017). Life history traits of a spadefood toad (*Pelobates cultripes*) population from a semiarid zone in the northeast of the Iberian Peninsula. *Herpetological Journal*. **27**. 57-61.

Pewsey, A., Neuhäuser, M., & Ruxton, G. D. (2013). Circular Statistics in R. *Oxford University Press.* 1–184.

Rebouças, R., Silva, H. R., Sanuy, D. & Solé, M. (2019). Sexual maturity and growth of male toads (*Rhinella ornata*): A comparison between insular and mainland populations, *Zoologischer Anzeiger*, **283**: 12–19. https://doi.org/10.1016/j.jcz.2019.07.002.

Rensch, B. (1950). Die Abhangigkeit der relativen Sexualdifferenz von der Körpergroße. *Bonner Zoologische Beiträge*, 1950, **1**: 58–69.

Roberto, I. J., Ribeiro, S. C., Bezerra, L., Carneiro, P. B. M. (2011). Amphibia, Anura, Hylidae, *Trachycephalus atlas* Bokermann, 1966: Distribution extension and geographic distribution map. *Check List*, **7**(3): 326-327.

Rodrigues, D. J., Uetanabaro, M. & Lopes, F. S. (2005). Reproductive patterns of Trachycephalus venulosus (Laurenti, 1768) and Scinax fuscovarius (Lutz, 1925) from the Cerrado, Central Brazil. *Journal of Natural History,* **39**: 3217–3226, DOI: 10.1080/00222930500312244

Rozenblut, B. & Ogielska, M. (2005). Development and growth of long bones in European water frogs (Amphibia: Anura: Ranidae), with remarks on age determination. *Journal of Morphology*, **265**, 304–317.

RStudio, Team. (2023). *RStudio: Integrated Development for R. RStudio*, PBC, Boston, MA, http://www.rstudio.com/.

Ryser, J. (1988). Determination of growth and maturation in the common frog, *Rana temporaria*, by skeletochronology. *Journal of Zoology,* **216**, 673–685.

Sá, F. P. de, Consolmagno, R. F., Muralidhar, P., Brasileiro, C. A., Zamudio, K. R., & Haddad C. F. B. (2020). Unexpected reproductive fidelity in a polygynous frog, *Science Advances*, **6** (33).

Stănescu, F., Marangoni, F., Reinko, I. & Dan, C. (2016). "Life history traits of a Neotropical microhylid (*Dermatonotus muelleri*, Boettger 1885) from the Arid

Chaco, Argentina." ("(PDF) Life history traits of a Neotropical microhylid (Dermatonotus ...") *Herpetological Journal.* **26.**

Sebens, K. P. (1987). The ecology of indeterminate growth in animals. *Annual Review of Ecology and Systematics*, 371–407.

Shine, R. (1988): The evolution of large body size in females: a critique of Darwin's ''fecundity advantage'' model. *The American Naturalist* **131**: 124–131.

Shine, R. (1989): Ecological causes for the evolution of sexual dimorphism: a review of the evidence. *Quarterly Review of Biology* **64**: 419–461.

Silva, L.A., Carvalho, P.S., Pereira, E. A., Fadel, R. M., Dantas, S. P., Brandão, R. A., Santana, D. J. (2020). Richness, diversity patterns, and taxonomic notes of amphibians from the Tocantins state. *Biota Neotropica.* **20**(1): e20190838. http://dx.doi.org/10.1590/1676-0611-BN-2019-0838.

Sinsch, U. (2015). Review: Skeletochronological assessment of demographic life history traits in amphibians. *Herpetological Journal*, **25**, 5–13.

Sinsch, U., Oromi, N., & Sanuy, D. (2007). Growth marks in natterjack toad (*Bufo calamita*) bones: Histological correlates of hibernation and aestivation periods. *The Herpetological Journal*, **17**, 129–137.

Smirina, E. M. (1972a). Annual layers in bones of *Rana temporaria*. *Zoologichesky Zhurnal* **51**, 1529– 1534.

Smirina, E. M. (1994). Age determination and longevity in Amphibians. *Gerontology* **40**: 133–146.

Tessa, G., Crottini, Z., Giacoma, C., Guarino, F. M., Randria-nirina, J. E., & Andreone, F. (2017). Comparative longevity and age at sexual maturity in twelve rainforest frogs of the genera *Boophis, Gephyromantis*, and *Mantidactylus* (Anura: Mantellidae) from Madagascar. *Phyllomedusa: Journal of Herpetology,* **16**(1), 13–21. https://doi.org/10.11606/issn.2316-9079.v16i1p13-21

Trueb, L. (1970). *Evolutionary relationships of casque-headed tree frogs with co-ossified skulls* (family Hylidae). Univ. Kans. Publ. Mus. Nat. Hist. **18**, 547–716.

Vaz-Silva, W., Maciel, N.M, Nomura, F., Morais, A.R., Batista, V.G., Santos, D.L., Andrade, S.P., Oliveira, A.B., Brandão, R.A., Bastos, R.P. (2020). *Guia de identificação das espécies de anfíbios (Anura e Gymnophiona) do estado de Goiás e do Distrito Federal, Brasil Central* [online]. Curitiba: Sociedade Brasileira de Zoologia, Zoologia: guias e manuais de identificação series. https://doi.org/10.7476/9786587590011.

von Bertalanffy, L. (1938). A quantitative theory of organic growth (inquires on growth laws. II). Human Biology, **10**, 181–213.

Zhang, L., Lu, Y., Lu, X., & Chen, X. (2013). Age and growth examined by skeletochronology for the stream-dwelling frog *Feirana taihannicus* in central China. *Herpetological Journal*, **23**, 89–9.

Tables and figures

Table 1. Number of individuals of the three species in each age class (in years) and relative frequency (%) of presence of nuptial pads or egg mass.

	T. nigromaculatus			*T. atlas*			*T. mambaiensis*		
	Females	Males	Juveniles	Females	Males	Juveniles	Females	Males	Juveniles
Age 0+				1				1	
Age 1+		1 (0%)	2					2 (100%)	1
Age 2+	1 (0%)	3 (33,3%)	2		2 (50%)	3	1 (0%)	3 (25%)	
Age 3+	8 (28%)	3 (75%)		1 (50%)	3 (0%)		1 (100%)	3 (100%)	
Age 4+	3 (66,6%)	2 (100%)			2 (100%)		1 (100%)		
Age 5+	2 (0%)	3 (66,6%)		1 (0%)					
Age 6+		2 (50%)		1 (0%)					

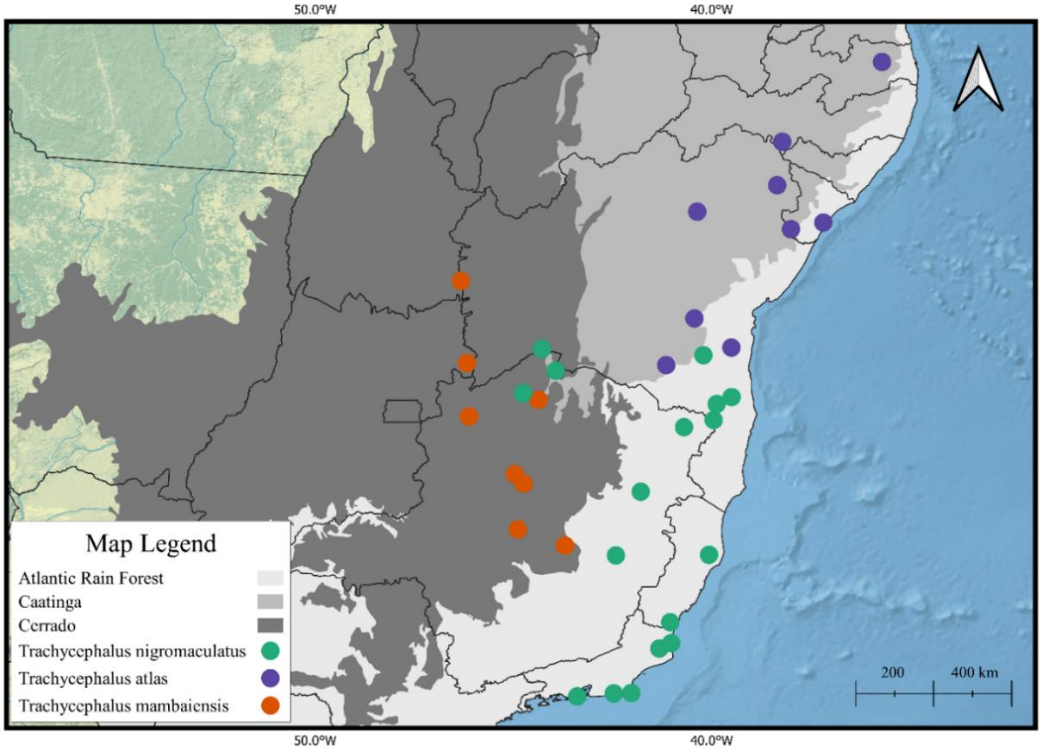

Figure 1. Map of localities of specimens collected during previous fieldwork.

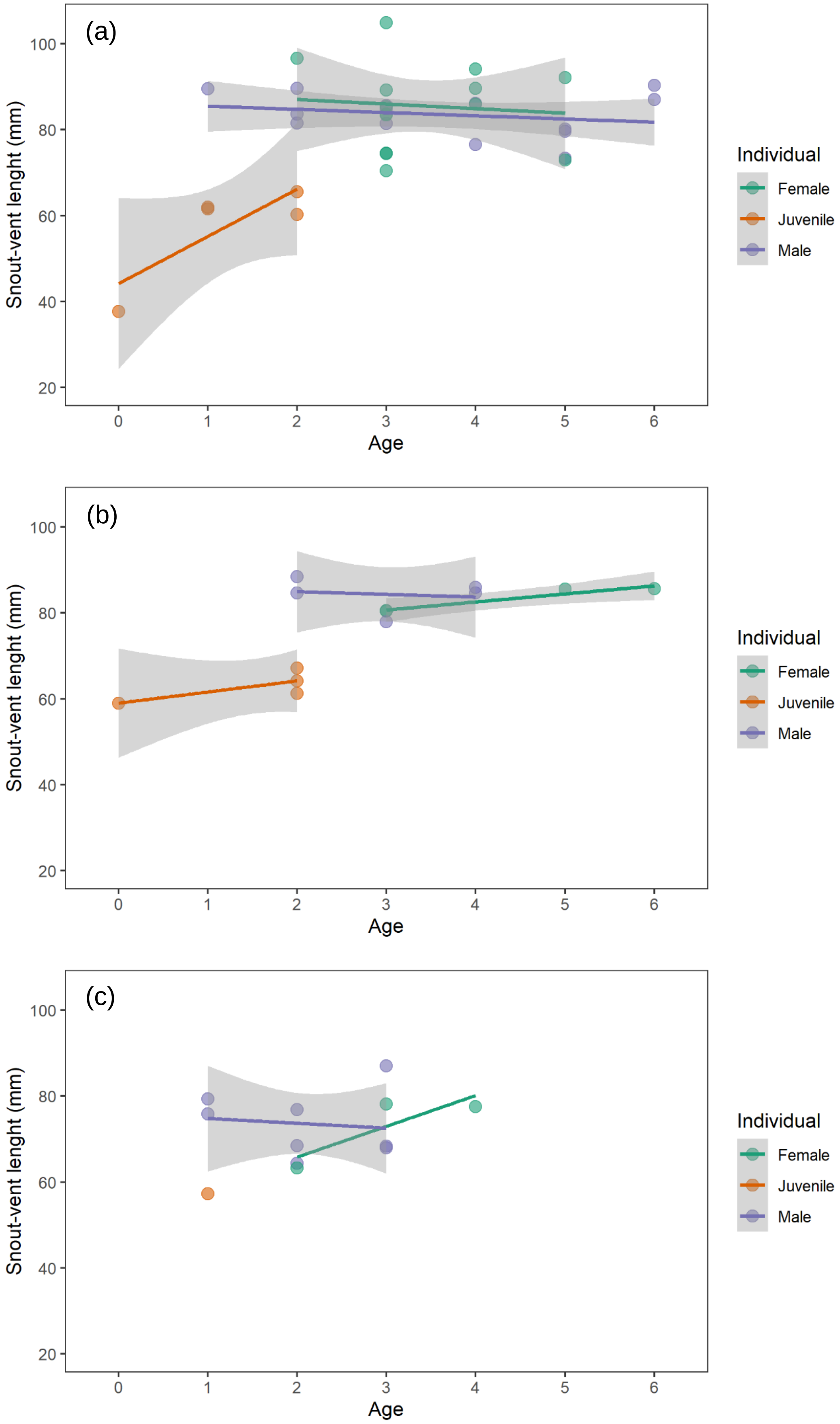

Figure 2. Correlation between age (in LAGs) and snout-vent length (mm) according to sex. (a) *T. nigromaculatus.* (b) *T. atlas.* (c) *T. mambaiensis.*

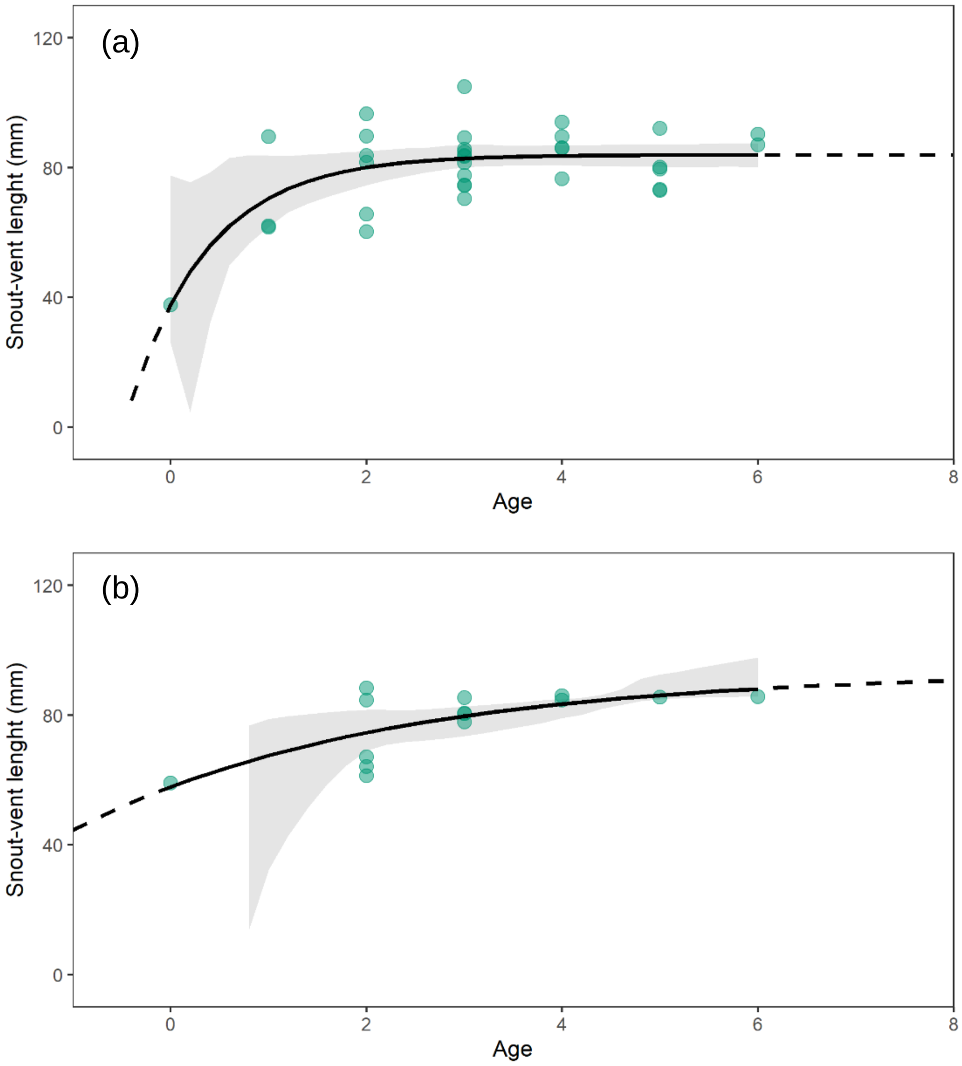

Figure 3. Growth curves of the two species according to Von Bertalanffy's growth curve. Lines represent mean and shaded areas 95% confidence intervals. (a) *T. nigromaculatus* (b) *T. atlas*.

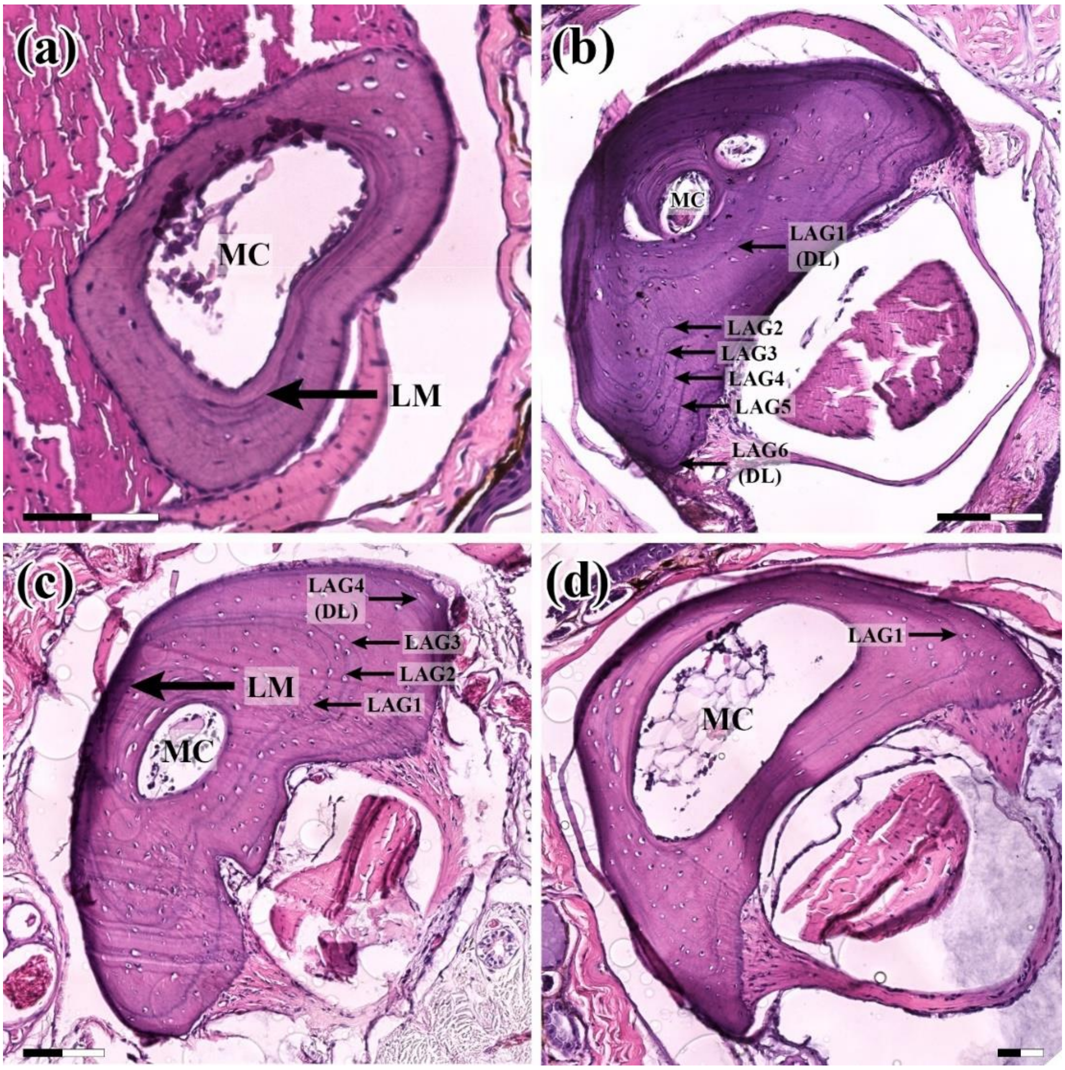

Figure 4. Photomicrography of phalanx cross sections and their histological interpretation. (A) *T.* atlas juvenile, without LAGs (B) *T. nigromaculatus* male, showing six LAGs (C) *T. atlas* male, showing four LAGs (D) *T. mambaiensis* male, showing one LAG. Abbreviations: DL = double line, LAG = line of arrested growth, LM = line of metamorphosis, MC = medullar cavity. Scale = 100 μm.